Arbeitsbericht NAB 20-08

TBO Bülach-1-1: Data Report

Dossier VI Wireline Logging and Microhydraulic Fracturing

March 2021

R. Garrard, J. Gonus, J. Desroches &
E. Bailey

National Cooperative
for the Disposal of
Radioactive Waste

Hardstrasse 73
P.O. Box 280
5430 Wettingen
Switzerland
Tel. +41 56 437 11 11

www.nagra.ch

nagra.

Arbeitsbericht NAB 20-08

TBO Bülach-1-1: Data Report

Dossier VI Wireline Logging and Microhydraulic Fracturing

March 2021

R. Garrard[2], J. Gonus[1], J. Desroches[1] & E. Bailey[1]

[1] GPCI Geneva Petroleum Consultants International
[2] Nagra

Keywords:
Bülach-1-1, Bülach-1-1B, Nördlich Lägern, TBO, deep drilling campaign, wireline logging, petrophysical logging, in situ testing, micro-hydraulic fracturing

National Cooperative for the Disposal of Radioactive Waste

Hardstrasse 73
P.O. Box 280
5430 Wettingen
Switzerland
Tel. +41 56 437 11 11

www.nagra.ch

Nagra Arbeitsberichte NAB ("Working Reports") present the results of work in progress that have not necessarily been subject to a comprehensive review. They are intended to provide rapid dissemination of current information.

This NAB aims at reporting drilling results at an early stage. Additional borehole-specific data will be published elsewhere.

In the event of inconsistencies between dossiers of this NAB, the dossier addressing the specific topic takes priority. In the event of discrepancies between Nagra reports, the chronologically later report is generally considered to be correct. Data sets and interpretations laid out in this NAB may be revised in subsequent reports. The reasoning leading to these revisions will be detailed there.

This Dossier was prepared by a project team consisting of:
R. Garrard (project management, lead author, QC)
J. Gonus (petrophysics QC, theoretical concepts, log analysis)
J. Desroches (MHF QC, theoretical concepts) and
E. Bailey (BHI QC, theoretical concepts, review)

Editorial work: Graphics and editing teams at Nagra

Petrophysical log graphic files were created using Geolog Emerson E&P Software - Emerson Paradigm and Terrastation.

The Dossier has greatly benefitted from technical discussions and initial review from Andreas Gautschi, and reviews by external and internal experts. Their input and work are very much appreciated!

Table of Contents

List of Tables

List of Figures

List of Appendices

Note: Only in the digital version of this report Appendices A – E can be found under the paper clip symbol.

1 Introduction

1.1 Context

To provide input for site selection and the safety case for deep geological repositories for radioactive waste, Nagra has drilled a series of deep boreholes in Northern Switzerland. The aim of the drilling campaign is to characterise the deep underground of the three remaining siting regions located at the edge of the Northern Alpine Molasse Basin (Fig. 1-1).

In this report, we present the results from the Bülach-1-1 borehole.

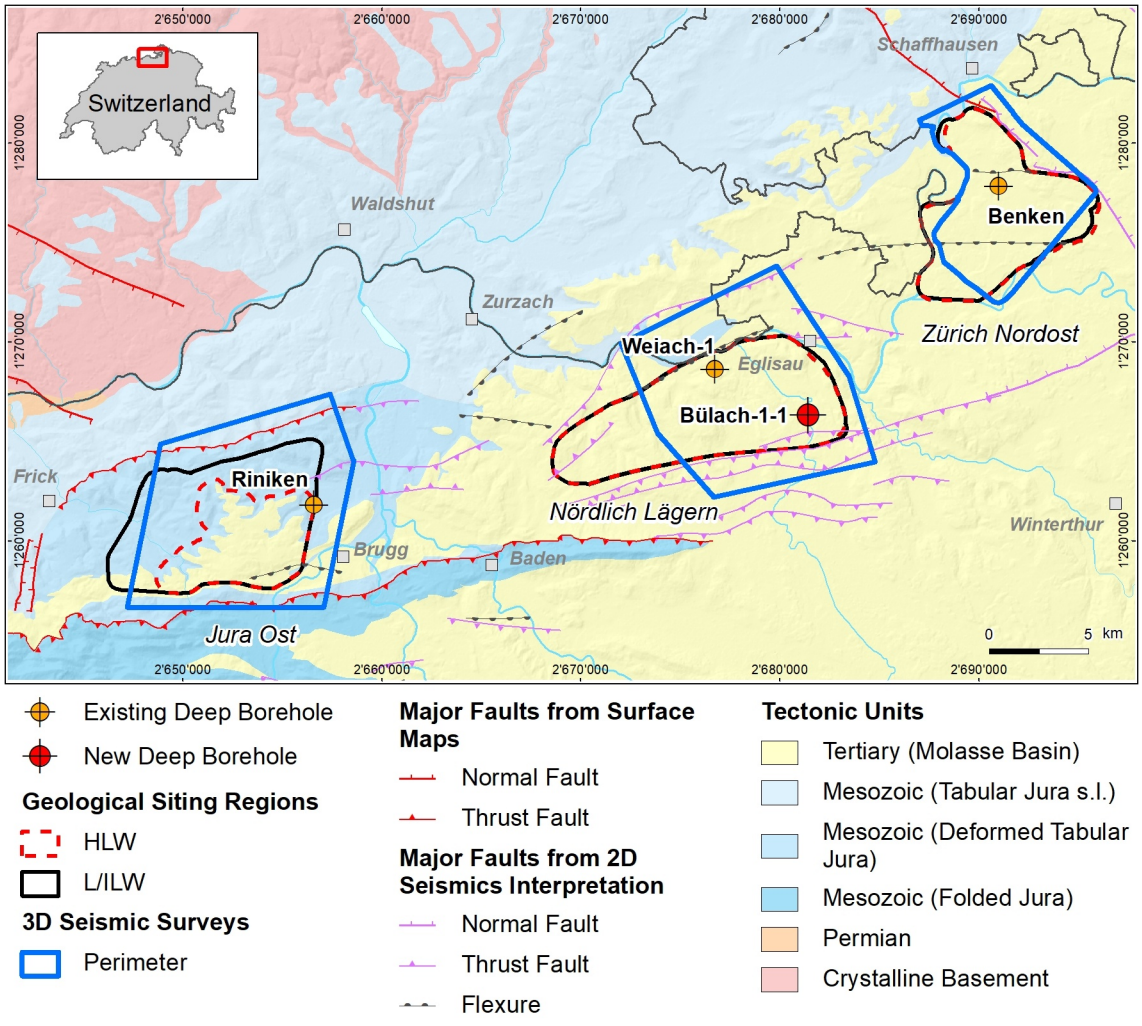

Fig. 1-1: Tectonic overview map with the three siting regions under investigation

1.2 Location and specifications of the borehole

The Bülach-1-1 (BUL1-1) exploratory borehole is the first deep borehole drilled within the framework of the TBO project. BUL1-1 is a vertical borehole. The drill site is located in the south-eastern part of the Nördlich Lägern siting region (Fig. 1-2). The borehole specifications are provided in Tab. 1-1. The lithostratigraphic profile and the casing scheme are shown in Fig. 1-3. Due to instabilities, the borehole was plugged back from 1'043.00 m to 918.70 m (cf. Dossier I). Resuming coring operations, a sidetrack was initiated with a kickoff point at 995.85 m. This sidetrack was labelled Bülach-1-1B (BUL1-1B). BUL1-1B reached the final depth of 1'370.19 m (MD core depth)[1]. For easier communication and labelling, the name BUL1-1 is generally used for the complete vertical borehole unless stated otherwise. Fig. 1-3 shows the combined lithostratigraphic profile of BUL1-1.

Tab. 1-1: General information about the BUL1-1 borehole

Location	Bülach (Canton Zürich/ZH), Switzerland
Siting region	Nördlich Lägern
Coordinates	2'681'446.028 / 1'266'298.472
Deep measurement elevation	389.62 m asl (top of rig cellar)
Elevation	389.62 m asl (top of rig cellar)
Borehole depth	1'370.19 m MD core depth
Drilling period	15 April 2019 – 27 November 2019 (spud – rig release)
Drilling company	Daldrup & Söhne AG
Drilling rig	Wirth B 152t
Drilling fluid	Water-based mud with varying amounts of Pure-Bore®, Pure-Bore® ULV, soda ash, sodium bicarbonate, xanthan gum

[1] *Measured depth (MD)* below top rig cellar along borehole trajectory. In all dossiers, depth refers to MD unless stated otherwise.

MD core depth refers to the depth marked on the cores. Note that petrophysical logs have not been shifted to core depth, hence MD log depth differs from MD core depth. The depth shift between core depth and log depth is documented in Dossier V, Appendix E-1.

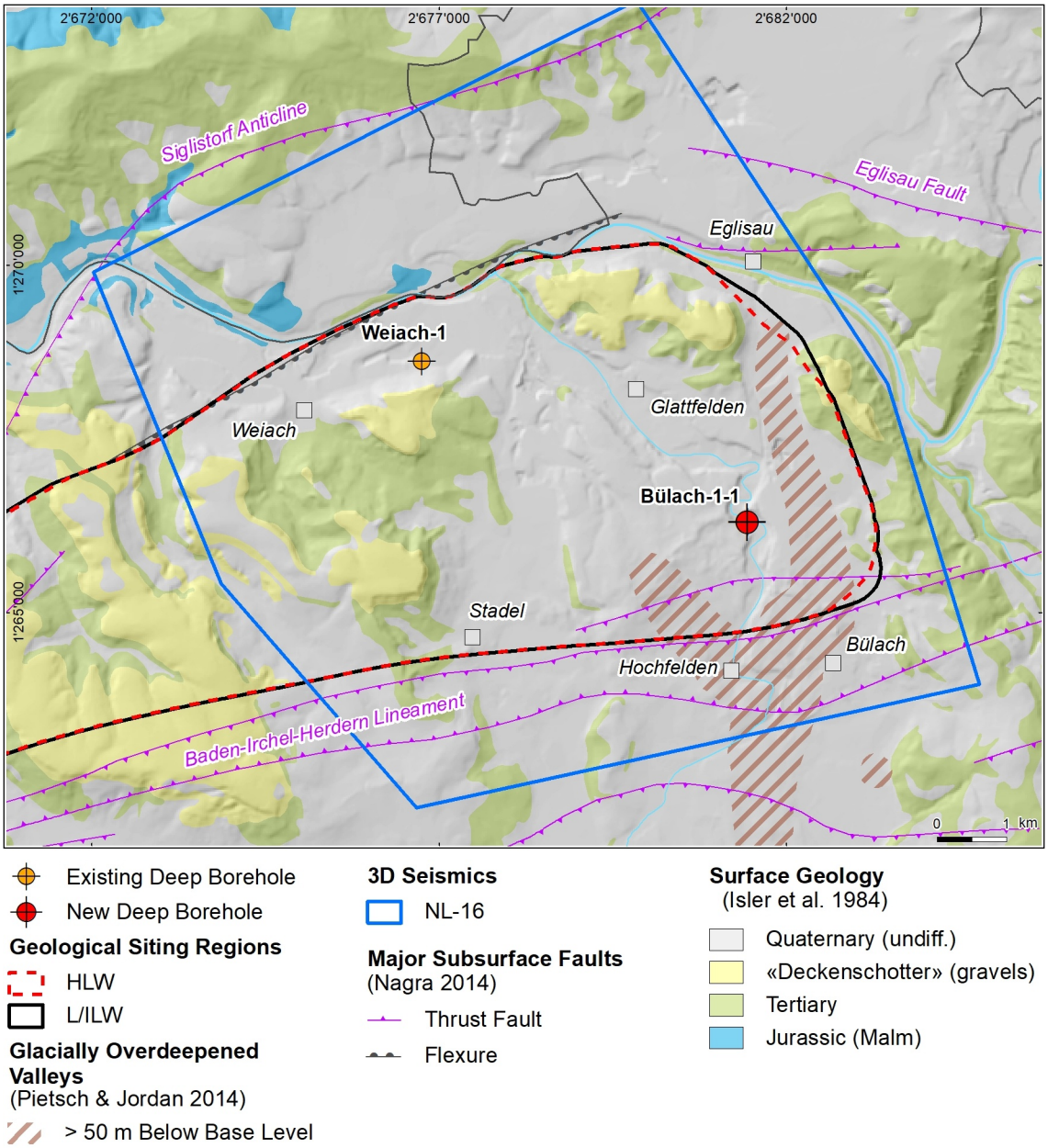

Fig. 1-2: Overview map of the investigation area in the Nördlich Lägern siting region with the location of the BUL1-1 borehole and the existing Weiach-1 borehole

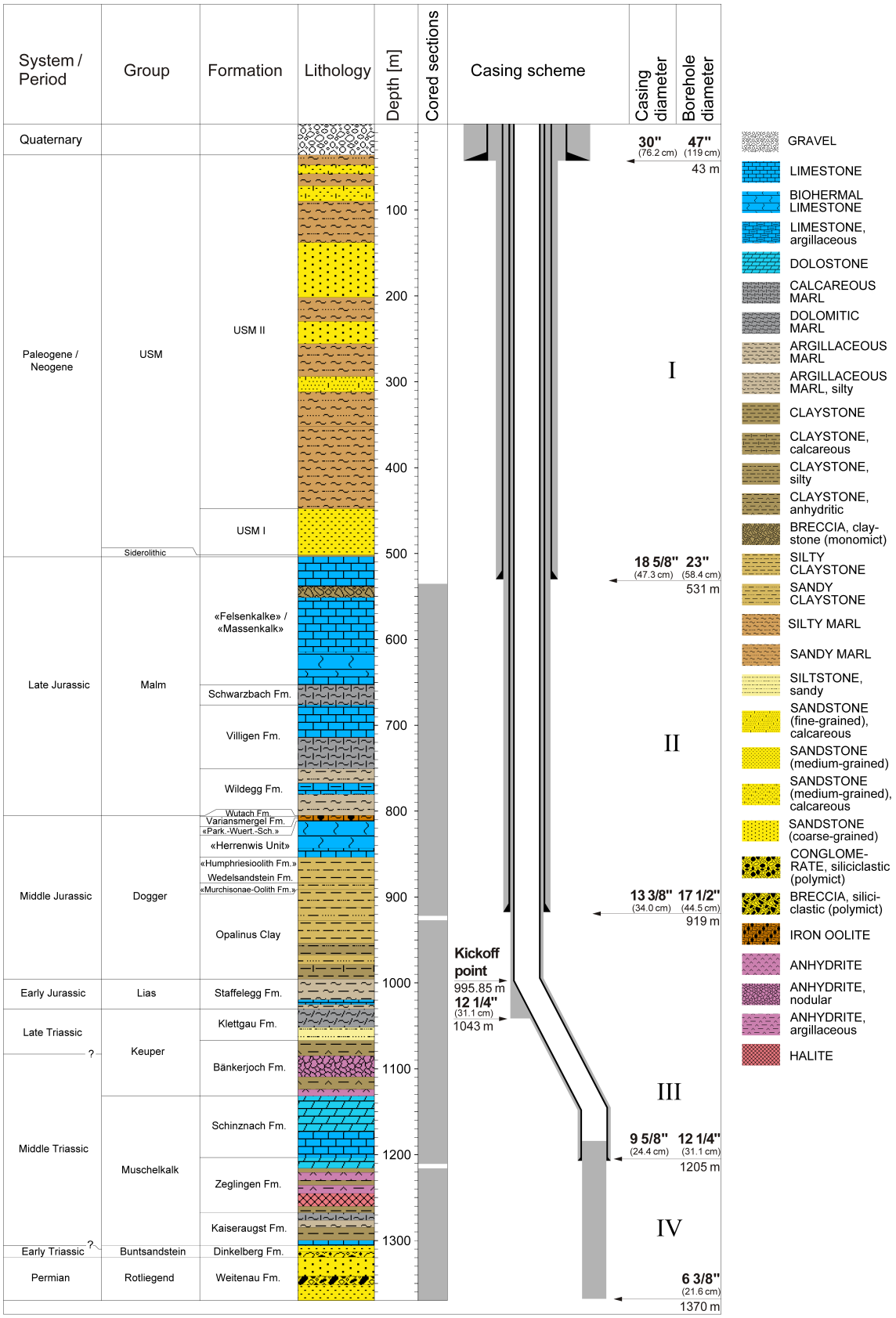

Fig. 1-3: Lithostratigraphic profile and casing scheme for the BUL1-1 borehole

1.3 Documentation structure for the BUL1-1 borehole

NAB 20-08 documents the majority of the investigations carried out in the BUL1-1 borehole, including laboratory investigations on core material. The NAB comprises a series of stand-alone dossiers addressing individual topics and a final dossier with a summary composite plot (Tab. 1-2).

This borehole documentation aims at early publication of the data collected in the BUL1-1 borehole. It includes the majority of the data available approximately one year after completion of the borehole. Some analyses are still ongoing (e.g. diffusion experiments, analysis of veins, hydrochemical interpretation of water samples) and will be published in separate reports.

The current borehole report will provide an important basis for the integration of datasets from different boreholes. The integration and interpretation of the results in the wider geological context will be documented later in separate geoscientific reports.

Tab. 1-2: List of dossiers included in NAB 20-08

Black marks the dossier at hand.

Dossier	Title	Authors
I	TBO Bülach-1-1: Drilling	M. Ammen & P.-J. Palten
II	TBO Bülach-1-1: Core Photography	D. Kaehr & M. Gysi
III	TBO Bülach-1-1: Lithostratigraphy	P. Jordan, H. Naef, P. Schürch, M. Schwarz, T. Ibele, R. Felber & M. Gysi
IV	TBO Bülach-1-1: Microfacies, Bio- and Chemostratigraphic Analysis	S. Wohlwend, H.R. Bläsi, S. Feist-Burkhardt, B. Hostettler, U. Menkveld-Gfeller, V. Dietze & G. Deplazes
V	TBO Bülach-1-1: Structural Geology	A. Ebert, L. Gregorczyk, E. Hägerstedt & M. Gysi
VI	TBO Bülach-1-1: Wireline Logging and Microhydraulic Fracturing	R. Garrard, J. Gonus, J. Desroches & E. Bailey
VII	TBO Bülach-1-1: Hydraulic Packer Testing	R. Schwarz, L. Schlickenrieder & T. Vogt
VIII	TBO Bülach-1-1: Rock Properties, Porewater Characterisation and Natural Tracer Profiles	M. Mazurek, L. Aschwanden, L. Camesi, T. Gimmi, A. Jenni, M. Kiczka, U. Mäder, D. Rufer, H.N. Waber, P. Wanner, P. Wersin & D. Traber
IX	TBO Bülach-1-1: Rock-mechanical and Geomechanical Laboratory Testing	E. Crisci, L. Laloui & S. Giger
X	TBO Bülach-1-1: Petrophysical Log Analysis	S. Marnat & J.K. Becker
	TBO Bülach-1-1: Summary Plot	Nagra

1.4 Scope and objectives of this dossier

This dossier describes the acquisition, quality control and results of the Petrophysical Logging (PL) and Micro-Hydraulic Fracturing (MHF) wireline logging measurements performed in the BUL1-1 borehole and its BUL1-1B side-track.

Petrophysical log measurements were acquired in open borehole conditions (no casing) with wireline conveyed logging tools to determine continuous profiles across the borehole of physical and chemical properties of the formation, including its mineralogy, clay types, porosity, fluid content, and acoustic properties. Petrophysical logs were further acquired to obtain high-resolution circumferential images of the borehole wall, as well as to measure borehole physical parameters such as its geometry, mud resistivity and mud temperature. In addition to the open hole logs, temperature logs were acquired post completion to measure the undisturbed mud temperature.

A series of in-situ stress measurements were performed using the micro-hydraulic fracturing technique to estimate the orientation and magnitude of the earth stress at different depths. The objectives of the MHF testing program were to provide estimates of the in-situ stress state in the Opalinus Clay potential rock host and adjacent rock formations and provide calibration points for mechanical earth models (MEM) of the rock mass (1D, 3D).

Except for the first two runs, all PL and MHF testing were performed by the wireline logging company Schlumberger (SLB). Geneva Petroleum Consultants International (GPCI) were responsible for planning wireline operations, technical supervision at the worksite, quality assurance and control (QA-QC) of data, database management and general wireline logging support.

This dossier is organised as follows:

- Chapter 2: The sequence of events for PL and MHF testing operations, and associated log/data coverage is provided.
- Chapter 3: The QA-QC procedure used to assess the quality of the petrophysical logs is detailed. A continuous profile of each log across the entire measured depth of the borehole is quality-controlled, corrected and spliced together to generate a quality-controlled composite log. The results of the composite log are discussed. The composite log will then be used as the final log data for input into further data analysis processes such as formation evaluation (e.g. Stochastic Petrophysical Log Analysis described in Dossier X), calibration with seismic data, and integration with sedimentology and structural geology data (from cores, cuttings, adjacent boreholes, and regional geology).
- Chapter 4: Although Borehole Imagery (BHI) logs were acquired as a part of petrophysical logging, the objectives of BHI are related to both Structural Geology (analysis of image features described in Dossier V) and MHF (firstly the selection of stations for MHF stress measurements, then the analysis of fractures induced by MHF tests). Thus, the QC, processing and interpretation processes of BHI are described in a chapter separate from the QA-QC procedures of the other petrophysical logs in Chapter 3.
- Chapter 5: MHF test procedures and preliminary results are presented.
- Finally, this report includes a set of appendices, where spliced PL, BHI and MHF data can be found.

2 Wireline logging and testing operations

The Bülach-1-1 (BUL1-1) borehole was planned in 4 drilling sections (also commonly referred to as phases). After installation of the 30" outer diameter (OD) standpipe, Section 1 was drilled and logged in the 23" drill bit size. Sections 2 through 5 were continuously cored using the 6 3/8" core bit and subsequently logged/tested. After wireline logging operations in each section were complete, the borehole was reamed (opened up) to 17 1/2" (Section 2) and 12 1/4" (Sections 3 and 4) to accommodate the 13 3/8" and 9 5/8" OD casing tubulars, respectively. Due to unstable borehole conditions in the lower Opalinus Clay, in Section 3 the original borehole was cemented in the interval between 918.7 and 1'043 m MD (core depths). A side-tracked borehole (BUL1-1B) kicked off at 995.85 m MD (core depth). This side-tracked section was renamed Section 4, and an additional Section 5 was added to the bottom section of the side-tracked borehole. Once open borehole logging/testing operations were complete, the borehole was backfilled with cement up to 1'185 m MD (inside the 9 5/8" OD casing). Three post-completion, petrophysical logs were acquired to measure the undisturbed mud temperature. Detailed descriptions of the borehole design and mud conditions at time of logging and testing are included in the excel Composite Report (Appendix A), under the worksheets entitled 'Borehole design' and 'Hole & Mud Conditions'. Additional details about borehole configuration, casing and cementing scheme and mud parameters can be found in Dossier I.

Wireline logging and testing operations were divided into the following groups of activities:

- Petrophysical Logging (PL)
- Micro-Hydraulic Fracturing (MHF)
- *Technical Logging (TL)*
- *Vertical Seismic Profiling (VSP)*

Petrophysical logs are continuous measurements (recorded every half foot or approximately 15 cm) of mineralogy and physical properties of formation rocks, their contained fluids, and the borehole environment between the wireline conveyed logging tool sensors and the borehole wall. Petrophysical logs were acquired with conventional and advanced wireline-conveyed logging tools. Conventional tools measured Depth (measured depth [MD], or log depth, that is the depth reference for all wireline measurements), Total Gamma Ray (naturally occurring gamma radiation), Spontaneous Potential (electric potential difference between the formation and an electrode at surface), Temperature, Caliper (measurement of the borehole diameter), Inclinometer (measurement of the borehole trajectory), as well as the standard "quad combo" tools: Resistivity (electrical resistivity at different depth of investigation in the formation), Sonic (compressional and shear wave slowness), Density (measurement of the bulk density and the photoelectric factor), and Neutron (measurement of the neutron hydrogen index, a proxy of porosity, as well as the sigma capture cross-section). Advanced tools measured the Spectral Gamma Ray (potassium, thorium and uranium contributions to the total naturally occurring gamma radiation), Elemental Spectroscopy, and Micro-resistivity and Ultrasonic borehole images. These logging tools and their main measurements are described in detail in the subsequent Chapter 3 – Petrophysical Logging and Chapter 4 – Borehole Imagery.

MHF involves using wireline-conveyed testing equipment to initiate and analyse the characteristics of micro-hydraulic fractures to estimate the current stress state in the rock formation at the 1 m scale. Tests were conducted using the SLB Modular Formation Dynamics Tester (MDT), which uses a straddle packer module, surface-controlled valves, pressure gauges and a downhole pump to initiate and propagate fractures at predefined discrete depths. MHF tests are described in Chapter 5 – Microhydraulic fracturing.

As well as PL and MHF operations, wireline operations also included Technical Logging (TL) and Vertical Seismic Profiling (VSP). TL acquired data on the physical properties of the open borehole (geometry and trajectory) and the permanent casing installation. The borehole geometry was measured using calipers for both assessing the borehole condition (breakouts/washouts present) and determining the volume of cement needed for casing installations. The borehole inclination and azimuth were measured to confirm the borehole verticality and identify its trajectory. To assess the quality of the cement behind the casing Cement Bond Logs (CBL) were acquired using a sonic tool. Borehole deviation surveys, cement volume calculations and CBL logs are described in Dossier I. VSP acquired high resolution borehole seismic measurements used for correlation with, and enhancement of, surface seismic data. VSP will be addressed in separate document. TL and VSP are not described further in this report.

A summary of all wireline logging and testing activities carried out in BUL1-1 borehole is given in Tab. 2-1. Fig. 2-1 depicts graphically the log coverage for the PL and MHF testing campaigns. In total, 5 PL and 3 MHF testing campaigns were undertaken. Open hole PL was conducted in all sections of BUL1-1, whilst MHF testing was only conducted in Sections 2, 4 and 5. PL and MHF data acquisition was limited in the host rock of the Opalinus Clay (Sections 3 and 4) owing to the unstable borehole and the subsequent cement sheath which ultimately voided most log measurements. A more detailed analysis of the log measurement coverage is provided in Chapter 3.

Details of the logging runs, logging dates, wireline logging company, logging interval, logging suite and principal measurements acquired for PL and MHF operations are provided in Tab. 2-2. Mnemonics for each tool in the logging suite listed in this table are given in Tab. 2-3.

Tab. 2-1: Logging and testing activities during drilling of the BUL1-1 borehole

Drilling phase / section	**Borehole diameter TD**	**Permanent casing size** **Casing shoe depth**	**Start date**	**End date**	**Coring**	**Technical logging**	**Petrophysical logging**	**Micro-hydraulic fracturing**	**Vertical seismic profiling**	**Comments**
1	23" 531.5 m	18 5/8" 530 m MD	15.04.2019	17.05.2019		×	×			
2	17 1/2" 920 m	13 3/8" 18.17 m MD	17.05.2019	15.08.1019	×	×	×	×	×	
3	12 1/4" 1'043 m	n/a	15.08.1019	25.09.2019	×		×			Phase abandoned and side-tracked due to borehole instability
4	12 1/4" 1'211 m	9 5/8" 1'205 m MD	25.09.2019	12.11.2019	×	×	×	×		KOP 995.85 m MD (core depth)
5	6 3/8" 1'370 m	n/a	12.11.2019	24.11.2019	×		×	×	×	

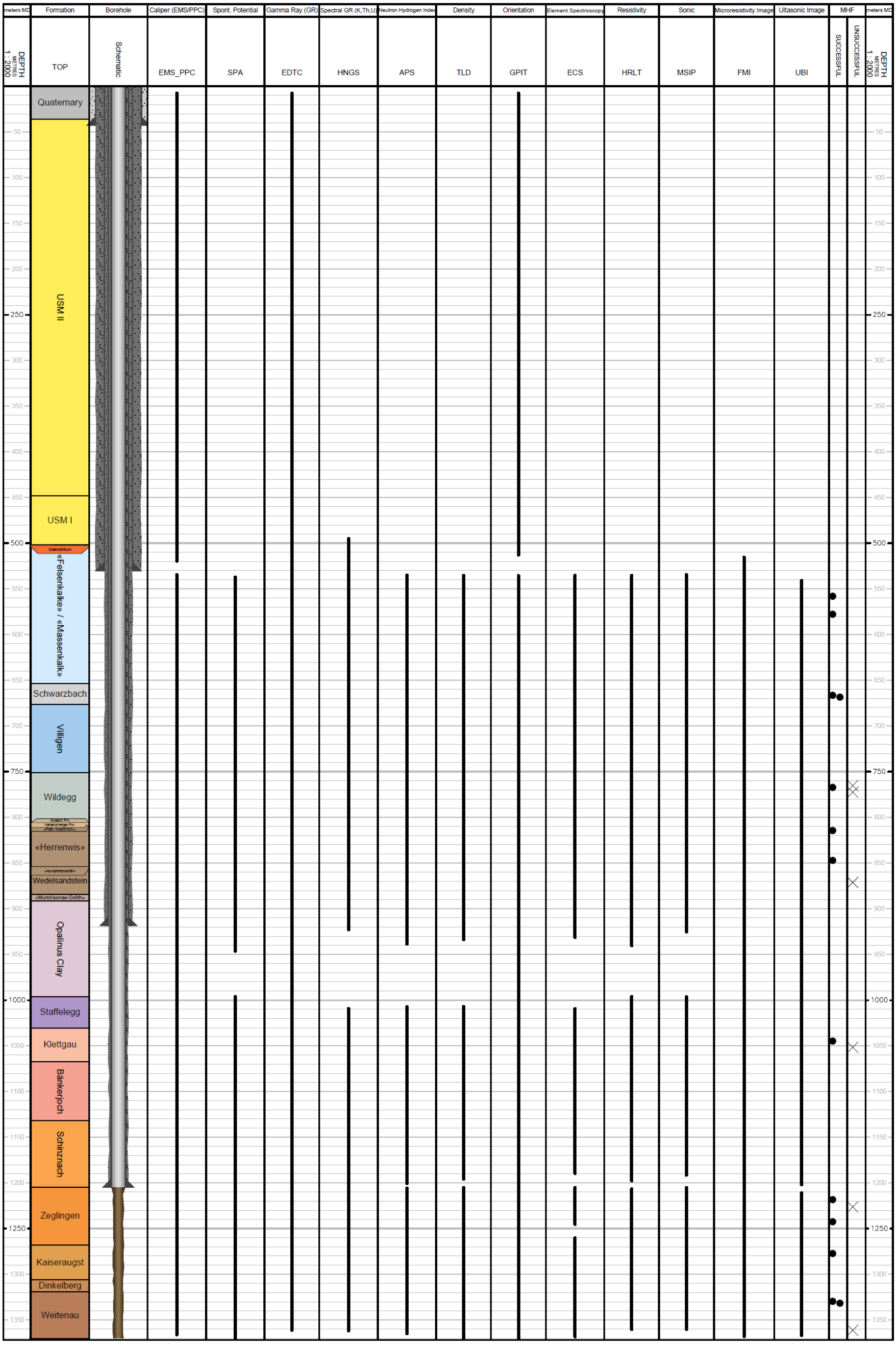

Fig. 2-1: Petrophysical log and MHF testing coverage at a scale of 1:2'000

Tab. 2-2: Logging and testing sequence of events

Phase / Section	Run	Operation	Logging date	Contractor	Logging interval (m MD)	Logging suite (see list of abbreviations)	Measurements																Remarks
							Gamma ray	Resistivity	Micro-resistivity	Density	Sonic	Neutron hydrogen index	Sigma capture cross section	Photoelectric factor	Spontaneous potential	Borehole imaging	Caliper	Spectral gamma ray	Elemental spectroscopy	Inclinometer	Temperature	MHF	
1	1.1.1	PP L	08.05.2019	SEMM	519.9 to 7.7	TENS/COMP-GR-INC/AZ-FWS-CAL-PRESS/TEMP	×				×						×			×			Bad sonic data (large hole)
	1.1.2	PP L	08.05.2019	SEMM	518.6 to 42.3	GR-DEN-TENS/COMP	×			×				×									Bad density-PEF data (large hole)
2	2.3.1	PP L	05.07.2019	SLB	950.9 to 495.6	FMI-EMS-EDTC-LEH.QT	×									×	×			×	×		First run in hole for depth reference
	2.3.2		05.07.2019	SLB	949.8 to 495.5	SP-EMS-APS-TLD-MCFL-EDTC-LEH.QT	×		×	×		×	×	×	×						×		
	2.4.1		06.07.2019	SLB	940.5 to 507.2	HRLT-EMS-ECS-HNGS-EDTC-LEH.QT	×	×									×	×	×		×		
	2.4.2		06.07.2019	SLB	943.3 to 532.5	UBI-GPIT-PPC-MSIP-PPC-EMS-EDTC-LEH.QT	×				×					×	×			×	×		
	2.4.3	MHF	07.07.2019	SLB	N/A	MRSC-MRSC-MRSC-MRPA-MRSC-MRPA-MRPO-MRSC-EDTC-LEH.QT																×	Run aborted
	2.5.1	MHF	08.07.2019	SLB	N/A	MRSC-MRSC-MRSC-MRPA-MRSC-MRPA-MRPO-MRSC-EDTC-LEH.QT																×	Run aborted
	2.6.1	PP L	12.07.2019	SLB	941.7 to 530.7	UBI-GPIT-PPC-EMS-EDTC-LEH.QT	×									×	×			×	×		
	2.6.2	MHF	12.07.2019	SLB	10 stations	MRSC-MTPO-MRSC-MRSC-MRSC-MRPA-MRSC-MRPA-MRSC-MRSC-MRPO-MRSC-EDTC-LEHQT																×	7 successful tests out of 10
	2.6.3	PP L	14.07.2019	SLB	941.1 to 526.7	FMI-EMS-EDTC-LEH.QT	×									×	×			×	×		Post-MHF FMI
3	3.1.1	PP L	27.06.2019	SLB	948.8 to 848.0	PPC-MSIP-PPC-GPIT-PPC-EDTC-LEH.QT	×				×						×			×			
	3.1.2		27.06.2019	SLB	946.7 to 838.0	EMS-EDTC-LEH.QT	×										×				×		
	3.2.1	PP L	12.09.2019	SLB	984.5 to 810.6	EMS-EDTC-LEH.QT	×										×				×		

Tab. 2-2: Cont.

Phase section	Run	Operation	Logging date	Contractor	Logging interval (m MD)	Logging suite (see list of abbreviations)	Measurements																Remarks
							Gamma ray	Resistivity	Micro-resistivity	Density	Sonic	Neutron hydrogen index	Sigma capture cross section	Photoelectric factor	Spontaneous potential	Borehole imaging	Caliper	Spectral gamma ray	Elemental spectroscopy	Inclinometer	Temperature	MHF	
3	3.3.1	PP L	17.09.2019	SLB	980.5 to 906.0	EMS-PPC-MSIP-PPC-GPIT-EDTC-LEH.QT	×				×						×			×	×		
	3.3.2		17.09.2019	SLB	982.1 to 916.4	SP-PPC-HRLT-EDTC-LEH.QT	×	×							×		×						
4	4.2.1	PPL	05.10.2019	SLB	1'074.3 to 868.8	FMI-EMS-EDTC-LEH.QT	×									×	×			×	×		Previous cement sheath affected logs at least down to 996 m MD
	4.2.2		05.10.2019	SLB	1'069.9 to 904.4	UBI-GPIT-EMS-EDTC-LEH.QT	×									×	×			×	×		
	4.2.3		05. – 06.10.2019	SLB	1'068.3 to 906.0	PPC-MSIP-PPC-GPIT-EMS-EDTC-LEH.QT	×				×						×			×	×		
	4.2.4		06.10.2019	SLB	1'065.0 to 904.6	APS-TLD-MCFL-EMS-GPIT-EDTC-LEH.QT	×		×	×		×	×	×			×			×	×		
	4.2.5		06.10.2019	SLB	1'065.8 to 904.6	ECS-HNGS-EMS-GPIT-EDTC-LEH.QT	×										×	×	×	×	×		
	4.2.6		06.10.2019	SLB	1'068.9 to 904.6	SP-GPIT-HRLT-EMS-EDTC-LEH.QT	×	×							×		×			×	×		
	4.3.1	PP L	17.10.2019	SLB	1'210.9 to 994.4	FMI-EMS-EDTC-LEH.QT	×									×	×			×	×		
	4.3.2		17.10.2019	SLB	1'202.0 to 1'039.4	UBI-GPIT-PPC-MSIP-PPC-EMS-EDTC-LEH.QT	×				×					×	×			×	×		
	4.3.3		17.10.2019	SLB	1'207.5 to 919.9	SP-APS-TLD-MCFL-PPC-EMS-EDTC-LEH.QT	×		×	×		×	×		×		×				×		
	4.3.4		18.10.2019	SLB	1'203.7 to 909.5	PPC-HRLT-ECS-HNGS- EMS-EDTC-LEH.QT	×	×									×	×	×		×		
	4.4.1	PP L	24.10.2019	SLB	1'209.4 to 902.8	EMS-EDTC-LEH.QT	×										×				×		
	4.4.2	MHF	25.10.2019	SLB	2 stations	MRPA -MRPA -MRSC-MRPO-MRSC.NJ-MRSC.J-MRSC.J-MRSC.NS-MRSC.NS-MRSC.G -MRPC-EDTA-EDTC-LEH.QT																×	1 successful test out of 2
	4.4.3	PP L	26.10.2019	SLB	1'108.1 to 1'009.4	FMI-EMS-EDTC-LEH.QT	×									×	×			×	×		Post-MHF

Tab. 2-2: Cont.

Phase section	Run	Operation	Logging date	Contractor	Logging interval (m MD)	Logging suite (see list of abbreviations)	Measurements																Remarks
							Gamma ray	Resistivity	Micro-resistivity	Density	Sonic	Neutron hydrogen index	Sigma capture cross section	Photoelectric factor	Spontaneous potential	Borehole imaging	Caliper	Spectral gamma ray	Elemental spectroscopy	Inclinometer	Temperature	MHF	
5	5.1.1	PP L	20.11.2019	SLB	1'370.5 to 1'131.3	FMI-EMS-EDTC-LEH.QT	×									×	×			×	×		
	5.1.2		20.11.2019	SLB	1'366.6 to 1'205.0	UBI-GPIT-EMS-EDTC-LEH.QT	×									×	×			×	×		
	5.1.3		20.11.2019	SLB	1'368.7 to 1'204.6	PPC-MSIP-PPC-GPIT-EMS-EDTC-LEH.QT	×				×						×			×	×		
	5.1.4		20.11.2019	SLB	1'370.2 to 1'199.1	SP-EMS-HRLT-EDTC-LEH.QT	×	×							×		×				×		
	5.1.5		21.11.2019	SLB	1'364.7 to 1'194.8	APS-EMS-EDTC-LEH.QT	×					×	×				×				×		
	5.1.6		21.11.2019	SLB	1'370.1 to 1'175.9	TLD-MCFL-EMS-EDTC-LEH.QT	×		×	×							×				×		
	5.1.7		21.11.2019	SLB	1'368.4 to 1'182.5	ECS-HNGS-EMS-EDTC -LEH.QT	×											×	×		×		
	5.1.8	MHF	21.11.2019	SLB	7 stations	MRPA-MRPA -MRSC.G-MRPO-MRSC.NJ-MRSC.J-MRSC.J-MRSC.NS-MRSC.NS-MRSC.XG -MRPC.XD-EDTA-EDTC-LEH.QT																×	5 successful tests out of 7
	5.1.9	PP L	23.11.2019	SLB	1'368.6 to 1'205.0	FMI-EMS-EDTC-LEH.QT	×									×	×			×	×		Post-MHF
	5.2.1	PP L	03.06.2020	SLB	1'181.0 to 0.0	EMS-EDTC-LEH.QT	×														×		Post completion
	5.3.1	PP L	15.12.2020	SLB	1'179.7 to 1.0	EMS-EDTC-LEH.QT	×														×		Post completion
	5.4.1	PP L	20.03.2021	SLB	1'179.8 to 10.3	EMS-EDTC-LEH.QT	×														×		Post completion

Tab. 2-3: Tool mnemonics and measurement details

Logging tool	**Wireline contractor**	**Mnemonic**	**Principal measurement**
4CAL	SEMM	4-arm caliper	Dual axis borehole measurements
APS	SLB	Accelerator porosity sonde	Epithermal neutron, sigma capture cross section of thermal neutrons
DEN	SEMM	Density	Bulk density, photoelectric factor
ECS	SLB	Elemental capture spectroscopy sonde	Measurement of the relative dry weight element concentration (e.g. Si, Ca, Fe, S, Ti, Gd, Cl and H) and mineralogical model
EDTC	SLB	Enhanced digital telemetry cartridge	Gamma ray measurement of the total natural radioactivity
EMS	SLB	Environmental measurement sonde	6-arm caliper, temperature and mud resistivity
FMI	SLB	Fullbore formation microimager	Microresistivity imaging tool (pad contact)
GPIT	SLB	General purpose inclinometry tool	Orientation/inclination of the borehole
GR	SEMM	Gamma ray	Gamma ray measurement of the total natural radioactivity
HNGS	SLB	Hostile natural gamma ray sonde	Spectral gamma ray measurements of natural radioactivity (potassium, thorium, uranium)
HRLT	SLB	High resolution laterolog array tool	Laterolog resistivity measurement at different depths of investigation
INC/AZ	SEMM	Inclination/azimuth	Orientation of the borehole
LEH.QT	SLB	Logging equipment head with tension	Head tension
LSS	SEMM	Long-spaced sonic	Compressional and shear wave slowness measurements (monopole source)
MCFL	SLB	Microcylindrically focused log	Measures the invaded zone resistivity (Rxo)
MRPA	SLB	Packer modules	Packer modules for MHF tests
MRPO	SLB	Pump out module	Downhole pump for MHF tests
MRSC	SLB	Sample chamber	Carrying fluid for MHF tests, sometimes filled with air, water, mud
MSIP	SLB	Modular sonic imaging platform (sonic scanner)	Compressional, shear and Stoneley wave slowness measurements (monopole and dipole sources); cement bond log
PPC	SLB	Power positioning calipers	4-arm caliper that gives dual axis borehole measurements

Tab. 2-3: Cont.

Logging tool	**Wireline contractor**	**Mnemonic**	**Principal measurement**
PRESS/ TEMP	SEMM	Pressure/temperature	Downhole temperature and pressure measurements
SP	SLB	Spontaneous potential	Measurement of electrical potential difference between the borehole and the surface
TENS/ COMP	SEMM	Tension/compression	Measures wireline tension and compression
TLD	SLB	Three-detector lithology density	Bulk density and photoelectric absorption factor measurement
UBI	SLB	Ultrasonic borehole imager	High-resolution acoustic (ultrasonic) images of the borehole

3 Petrophysical logging

3.1 Petrophysical logging tools and measurements

Below the main petrophysical measurements acquired and the downhole logging tools deployed are summarised. A detailed description of how the different tools measure the respective parameters and the underlying physics behind these measurements is not the focus of this report. Borehole imaging tools are described in Chapter 4.

- **Borehole deviation/orientation** (GPIT – General Purpose Inclinometry Tool). The GPIT outputs inclinometer measurements. Tool orientation is defined by three parameters: tool deviation, tool azimuth and relative bearing. Borehole trajectory is calculated from the inclinometer measurements. Inclinometer measurements serve to reference the oriented logs (e.g. borehole imagery and sonic dipole logs).
- **Caliper log** (EMS/PPC – Environmental Measurement Sonde/Powered Positioning Caliper). The caliper log uses several coupled pairs of mechanical arms (2 pairs with PPC, 3 pairs with EMS) to continuously measure the borehole shape in different orientations.
- **Density** (TLD – Three-detector Lithology Density). TLD is an induced radiation tool that measures the bulk density of the formation and the photoelectric factor (PEF). It uses a radioactive source to emit gamma photons into the formation. The gamma rays undergo Compton scattering by interacting with the atomic electrons in the formation. Compton scattering reduces the energy of the gamma rays in a stepwise manner and scatters the gamma rays in all directions. When the energy of the gamma rays is less than 0.5 MeV they can undergo photoelectric absorption by interacting with the atomic electrons. The flux of gamma rays that reach each of the detectors of the TLD is therefore attenuated by the formation, and the amount of attenuation is dependent upon the density of electrons in the formation, which is related to its bulk density. The bulk density of a rock is the sum of the minerals (solids) and fluids volumes (porosity) times their densities. Hence, the formation density tool is key for the determination of porosity, the detection of low-density fluids (gasses) in the pores and lithological identification. In addition, the TLD provides the photoelectric absorption index (Photoelectric factor – PEF), which represents the probability that a gamma photon will be photo-electrically absorbed per electron of the atoms that compose the material. The PEF characterises the mineralogy. TLD tool is housed in the High-Resolution Mechanical Sonde that also includes the Micro-Cylindrically Focused Log (MCFL) sonde, that measures the micro-resistivity or alternatively, the resistivity very close to the borehole wall (RXOZ). The bulk density was integrated over depth, to provide the overburden pressure or vertical stress (Sv).
- **Element Spectroscopy** (ECS – Elemental Capture Spectroscopy). The ECS is also an induced radiation tool with a radioactive neutron source. The ECS measures the concentration of a series of elements in the formation (Si, Ca, Fe, S, Ti, Gd, Cl, H) by analysing the gamma ray spectrum of back scattered gamma rays. Special processing techniques allow under certain circumstances the measurement of supplementary elements such as Al, Mg, K and Na. The element spectroscopy measurements are provided in dry weight elements. SLB uses an algorithm in the field to derive a model of dry weight fractions of minerals from the dry weight element concentrations: clay, clastics (Quartz-Feldspar-Mica – QFM), carbonates, anhydrite/gypsum, salt/evaporite, pyrite and matrix. Under certain circumstances, advanced models are able to discriminate limestone and dolomite from carbonates, as well to provide a more quantitative clay measurement. It is important to note that mineralogy model processing is qualitative and should be viewed as an indicator of lithology and not used in any quantitative analysis. Quantitative analysis of the ECS dry weight elements needs to be calibrated against core data. Dossier X details stochastic processing and interpretation of the

ECS dry weight proportions, combined with conventional petrophysical log response, to generate a quantified lithology determination.

- **Gamma Ray** (GR, from the EDTC – Enhanced Digital Telemetry Cartridge). This log measures the total naturally occurring gamma ray radioactivity in the formation rocks (potassium, thorium and uranium are the most common radioactive elements in Earth's crust), which can be used to determine the volume of clay minerals (that contains those elements). The GR log is not valid for clay determination if other minerals contain those elements in significant amount (e.g. potassic feldspars, organic matter). The GR is run with all logging runs because it is used for depth correlation between runs thanks to its excellent vertical resolution and character. Note this is not to be confused with the Spectral Gamma Ray which is a different tool detailed further below.
- **Neutron Hydrogen Index, commonly named neutron** (NHI, from the APS – Accelerator Porosity Sonde). A particular accelerator called a Minitron generates high energy neutrons (14 MeV) that are emitted into the formation. Elastic collisions with the atom nuclei slow down the neutrons, a process that is more efficient with nuclei whose mass is close to that of neutron, i.e., hydrogen (the lightest element). Five detectors count the neutrons back from the formation at different distances from the Minitron, allowing for an environmental compensation of the signal. The received signal is mostly (but not only, for example the carbon atoms bring a significant contribution) dependent on the hydrogen concentration in the formation, hence the Hydrogen Index (HI) measurement: the larger the count, the lower the HI and its uncertainty. The APS tool can measure both an epithermal HI (APLC curve) and a thermal HI (FPLC). The hydrogen content in rocks is mostly in the fluids contained within, generally water or hydrocarbons, which have a HI close to 1 v/v. Nevertheless, some fluids like gas and high salinity brines have a HI lower than 1 v/v and must be corrected for when interpreting the results. In addition, many hydrated minerals are encountered in sedimentary or crystalline rocks, e.g. clay minerals, gypsum, iron-hydroxides, coals, zeolites, micas and amphiboles. The NHI is commonly used to quantify the fluid volume (porosity) and as a lithological indicator (clay content, hydrogen-rich minerals), mostly in combination with the bulk density measurement.
- **Resistivity** (HRLT – High Resolution Laterolog array Tool). The HRLT measures electrical resistivities at different depths of investigation in the formation. When drilling mud filtrate invades the formation and it has a salinity that contrasts with that of the formation fluids (the chlorine ion Cl- changes significantly the resistivity of a medium), the resistivities provide an invasion profile. Processing allows the extrapolation of the resistivity measurements far into the formation providing the true formation resistivity, as well as close to the tool, providing the micro-resistivity or resistivity close to the borehole wall. Resistivity is used to interpret the saturation in water or hydrocarbons in pore spaces.
- **Sigma Formation Capture Cross-Section** (SIGF, from APS). In addition to the HI, the APS also measures the sigma formation capture cross-section (SIGF), that is defined as the relative ability of a material to "capture" or absorb free thermal neutrons. SIGF values vary widely with elements and it can be used to determine the mineralogy and formation fluid contents.
- **Sonic** (MSIP – Modular Sonic Imaging Platform, also named Sonic Scanner). The MSIP measures how fast compressional and shear waves travel in the formation. A pulse sound is emitted from several tool transmitters in all directions. Tool receivers record the waves after they have travelled through a known path in the formation to the borehole wall. Waves travel at different velocities in the drilling fluid (between the tool and the borehole wall) and in the formation. Subtracting the travel time recorded by the near transmitter-receiver pairs from the travel time recorded by far transmitter-receiver pairs provides the travel time spent in the formation only and thus discards the wave propagation in the fluid. Travel times are converted

to wave slowness logs (inverse of velocity) based on the tool geometry. Compressional and shear wave slowness are used to interpret porosity, aid in mineralogy determination, for geomechanical and rock strength properties and they serve as calibration for seismic surveys. Other wave propagation modes are also recorded by the MSIP (oriented shear waves, Rayleigh waves, Stoneley waves). Oriented shear waves can be used to analyse the acoustic anisotropy properties of the formation. The MSIP log products require processing of the raw data to detect the different wave arrivals and transform the multiple transmitter-receiver recordings into unique slowness logs. Field processing products are basic and advanced processing products, such as, the anisotropy analysis can be requested at a later stage.

- **Spectral Gamma Ray** (SGR, from the HNGS – Hostile Natural Gamma Ray Sonde). In addition to the total gamma ray, the HNGS measures the energy spectrum of the formation gamma rays. As the three main radioactive elements (potassium, thorium and uranium) are characterised by a different gamma energy, the tool can quantify those elements content. Those concentrations can be used to quantify potassium, uranium or thorium rich minerals (e.g. different clay minerals, potassic feldspars, organic matter, phosphates). HSGR log is the sum of potassium, thorium and uranium gamma ray contribution to the total spectral gamma ray. Note that the total gamma ray from the GR and SGR tools are not necessarily quantitatively equivalent because these tools use different detectors, technologies, tool housing and calibrations. HCGR log is the result of the HSGR log without the uranium contribution. The shading from HCGR to HSGR in log plots help identify zones that may contain organic matter or phosphates.
- **Spontaneous Potential** (SP). The SP log is a continuous measurement of the electric potential difference between an electrode in the SP tool and a surface electrode. Adjacent to shales, SP readings usually define a straight line known as the shale baseline. Next to permeable formations, the curve departs from the shale baseline; in thick permeable beds, these excursions reach a constant departure from the shale baseline, defining the "sand line". The deflection may be either to the left (negative) or to the right (positive), depending on the relative salinities of the formation water and the mud filtrate. If the formation-water salinity is greater than the mud-filtrate salinity (the more common case), the deflection is to the left. The movement of ions, essential to develop an SP, is possible only in rocks with some permeability, a small fraction of a millidarcy is sufficient. There is no direct relationship between the magnitude of the SP deflection and the formation's permeability or porosity.
- **Temperature** (TMP). The temperature log is acquired with the EMS tool that includes a temperature sensor. It is a measurement of the temperature in the borehole environment; thus it is largely influenced by the temperature of mud. Since the temperature is affected by material outside the casing, a temperature log is sensitive to not only the borehole but also the formation and the casing-formation annulus. Mud temperature is generally less than that of fluids in the formation, but the temperature of the static mud is assumed to converge to the formation temperature after an infinite time. In practice, temperature logs are acquired several times after the last mud circulation and the formation temperature is modelled based on the observed trend of temperature vs time at each depth. On one hand, the temperature log is interpreted by looking for larger scale anomalies, or departures, from a reference gradient. This can give indications for permeable zones with fluid flow or for flow barriers hindering cross formational flow. On the other hand, localised smaller scale anomalies may correspond to the entry of borehole mud in the formation or fluid flow from the formation to the borehole. The temperature log should be interpreted together with structural geology, hydrogeology, and the other logs (e.g. images, resistivity logs).

3.2 Log data quality

3.2.1 Quality control procedures

Quality control (QC) of log data is important to guarantee their accuracy, repeatability, traceability, relevance, completeness, sufficiency, interpretability, clarity and accessibility. The generic QC procedures that were followed for each log dataset are presented below.

1. Digital data in .dlis format are loaded into a petrophysics software (Paradigm – Geolog) and checked for completeness (are principal log channels, parameters and constants given?) and accessibility (Do the data load correctly when imported? Is the depth sampling rate steady and valid?).

2. Sufficient data: do the first and last readings correspond to the interval of logs laid-out in the work program?

3. Depth match is checked versus reference run. First run in hole is by convention the reference for subsequent runs. GR log of the EDTC tool is always used for depth correlation because it has excellent vertical resolution and sufficient character. Schlumberger depth matches data in the field but sometimes additional depth matching is required during QC. Such depth shifts are recorded in App. A6 - Table of depth shifts.

4. Are the calipers well calibrated? This is checked by comparing caliper measurements against the nominal inner diameter of the casing.

5. Borehole shape is checked: are there washouts? Is the borehole on gauge? Undergauge? Ovalised? Are there breakouts? When the borehole shape is not gauge, the log quality can be degraded.

6. Does the cable tension show any overpulls or stick and pull events? These events can cause a locally discontinuous depth log measurement and alter the tool positioning which impacts log quality.

7. Graphic files (log plots) are checked for completeness, consistency and accuracy. In particular, the following sections of the graphic files are checked:

   7.1 Header: e.g. logging date, run number, mud parameters

   7.2 Borehole sketch and size/casing record: hole bit sizes and depths, casing sizes, weight and depth

   7.3 Borehole fluids: accuracy of mud physical parameters

   7.4 Remarks and equipment summary: serial numbers of equipment, completeness and accuracy of remarks

   7.5 Depth control parameters: right depth control policy and log of reference

   7.6 Summary of run passes: top and bottom of pass, automatic bulk shift applied

   7.7 Log (content and display): mnemonics, description, unit, scale, colour and label of logs; display of logs, log quality control (LQC) or data copy indicator curves provided (if applicable)

7.8 Parameters are checked including channel processing and tool control: corrections or offsets applied to measurements, modes of acquisition, etc.

7.9 Calibration reports are checked for completeness and tolerances.

8. Data repeatability for main versus repeat passes (or downlog pass if applicable) is checked for a selection of important logs.

9. Were required environmental corrections applied with the correct parameter values (e.g. mud salinity, mud weight, drill bit size, tool standoff, pressure/temperature).

10. Were processing parameters correctly applied (e.g. ECS minerals model options, MSIP time windows, APS lithology conversions)

11. Data consistency is checked, including a comparison with logs from other runs via log plot and crossplots and the description of the cuttings for lithology. Are logs representative of expected lithologies and do they respond consistently?

12. Are orientation, accelerometer and magnetometer data accurate? This is essential for all datasets that need to be oriented (e.g. borehole imagery [FMI/UBI], dipole sonic).

13. Mud resistivity and borehole temperature are checked for repeatibility and checked against collected mud samples and thermometers in the logging head.

14. Quality of automatic picking on processing products (if applicable), e.g. compressional and shear wave slowness on semblance projections for sonic logs.

3.2.2 Bad hole flags

To complete the data QC process, bad hole flags were created to highlight zones where the log quality was degraded by 'bad hole' conditions and should be viewed with caution. The methodology is presented in Tab. 3-1 and explained in detail in App. A7- Bad hole flags.

Bad hole is a common issue with logging. It means that the borehole conditions are inadequate for obtaining optimum quality petrophysical logs that truly represent the formation that is being logged. The tools that either measure petrophysical properties in a space volume or must be in continuous contact with the borehole wall during logging (eccentered tools) are the most affected by bad hole. Washouts and rugose hole are the most common features that degrade the quality of the logs resulting for example in the underestimation of density and overestimation of sonic slowness.

Tab. 3-1: Bad hole flag methodology

Bad hole logic	**Logs used**	**Cutoff/method**
Overgauge flag	Caliper	Borehole diameter is greater than 115% of nominal drill bit size
Rugosity flag	Density correction (HDRA), acquired with TLD	The density correction log is calculated from the difference between the short- and long-spaced density measurements, an indicator of borehole rugosity and density quality. Density is not reliable when HDRA > 0.025 g/cm^3
Neutron standoff	Neutron standoff (STOF), acquired with APS	Neutron tool should be flush with borehole wall or have pre-determined physical standoff. If unintentional standoff, STOF > 0.35", badhole is flagged
Density-neutron flag	Density (RHOZ) and neutron (APLC)	Systematic identification of outliers in density-neutron crossplot and comparison with analogue data from adjacent boreholes (e.g. Benken).

3.3 Composite log generation

The objective of the composite log dataset is to provide a traceable quality controlled, edited, corrected, and merged dataset for all petrophysical logging data recorded across the entire length of the borehole. Petrophysical tools acquire many logs that are not directly related to petrophysical properties but are needed to control that the tool sensors worked well (e.g. mechanical or electronics status of the sensors). In addition, some logs are acquired several times in a section (e.g. GR, Temperature). GPCI selects a collection of the most relevant logs for formation evaluation, correlation and calibration with core or seismic data. Some 65 representative logs are thus extracted for each borehole section. These logs are:

1. quality controlled (procedures in Section 3.2.1)
2. edited e.g. to keep data points that are true responses of the rocks formation
3. further corrected for the borehole environment when the logging provider could not apply all the required corrections (e.g. ECGR_EDTC log of Schlumberger that is corrected to GR_COR by GPCI)
4. merged into composite logs that cover the entire or most of the borehole
5. The generated composite log dataset is generated and delivered in standard digital (LAS – Log ASCII Standard) and graphic (PDF log plot) format.

A more detailed procedure for the generation of the composite log is detailed in the next subchapter. In addition, a complete report in Excel format is provided (see Appendix A) which details all relevant information about the logs and the acquisition runs. App. A5 – Composite log worksheet specifically details how the composite log dataset was generated through merging techniques.

3.3.1 Generic process

The following steps were conducted to generate composite log dataset:

1. A bit size log was generated according to the borehole design at the time of logging.
2. Logs were depth-shifted as applicable (see App. A6 - Table of depth shifts).
3. First and last readings were edited to remove values acquired before the tool sensors started reading the borehole (e.g. constant values just before/after the sensor is switched off/on) and to disregard artefacts (e.g. spectral gamma ray).
4. Bad hole and cement flags were created based on advanced log analysis to highlight zones where the log quality was affected by bad hole conditions.
5. Total gamma ray log (ECGR_EDTC) from the EDTC tool were normalised to account for attenuated readings in cased hole intervals using open hole readings from the same formation as the cased hole interval as proxies. The corrected gamma ray log is renamed GR_COR.
6. Spectral gamma ray log readings (HNGS tool) were discarded when formation was activated by the APS minitron. I.e.,when the APS was run prior to the HNGS.
7. All logs that were not valid in the cased hole were discarded (e.g. bulk density, neutron porosity, sonic, resistivity, element spectroscopy, spectral gamma ray).
8. Invalid ECS responses according to LQC curves were removed, e.g. in salt bed from 1'245 to 1'260 m MD.
9. Poor quality sonic slowness data (DTCO, DTSM) caused by imprecise automatic picking were removed and interpolated where applicable.
10. The edited and corrected logs from each section were merged. Merging points were chosen carefully to optimise log coverage and composite log consistency. See App. A5 - Composite log.
11. Standardised log names and units were used.
12. Logs acquired at higher resolution (e.g. RHO8, PEF8 have sample rates 0.0508 m – 1/6 ft) were resampled to the standard rate of 0.1524 m (1/2 ft). This is particularily important for LAS digital files, which cannot support mixed sample rates.
13. Final log plots at a scale of 1:200 m MD and 1:1'000 m MD were produced in PDF graphic file format along with digital data in LAS format.

Tab. 3-2 lists and describes all the log curves/channels that are provided in the composite log set.

Tab. 3-2: Composite log LAS channel listing

Curve/channel	**Units**	**Description**
DEPTH	M	
APLC	V/V	Near/array Corrected Limestone Porosity
BS	IN	Bit Size
DEVI	DEG	Borehole deviation
DTCO	US/F	Delta-T Compressional
DTSM	US/F	Delta-T Shear
DTST	US/F	Delta-T Stoneley
DWAL_WALK2	W/W	Dry Weight Fraction Pseudo Aluminum (SpectroLith WALK2 Model)
DWCA_WALK2	W/W	Dry Weight Fraction Calcium (SpectroLith WALK2 Model)
DWCL_WALK2	KGF/KGF	Dry Weight Fraction Chlorine Associated with Salt (SpectroLith WALK2 Model)
DWFE_WALK2	W/W	Dry Weight Fraction Iron + 0
DWGD_WALK2	PPM	Dry Weight Fraction Gadolinium (SpectroLith WALK2 Model)
DWHY_WALK2	KGF/KGF	Dry Weight Fraction Hydrogen Associated with Coal (SpectroLith WALK2 Model)
DWSI_WALK2	W/W	Dry Weight Fraction Silicon (SpectroLith WALK2 Model)
DWSU_WALK2	W/W	Dry Weight Fraction Sulfur (SpectroLith WALK2 Model)
DWTI_WALK2	W/W	Dry Weight Fraction Titanium (SpectroLith WALK2 Model)
FLAG_BADHOLE_ND		Neutron Density Crossplot Badhole flag
FLAG_BADHOLE_OVERGAUGE		Overgauge Borehole Badhole Flag
FLAG_BADHOLE_RUGO		Rugose Borehole Badhole Flag
FLAG_BADHOLE_STOF		Neutron Porosity Standoff Badhole Flag
FPLC	V/V	Near/Far Corrected Limestone Porosity
GR_COR	GAPI	Total natural radioactivity corrected
HAZI	DEG	Borehole azimuth
HCGR	GAPI	HNGS Computed Gamma Ray
HDAR	IN	Hole Diameter from Area
HDRA	G/C3	Density Standoff Correction
HFK	%	HNGS Formation Potassium Concentration
HSGR	GAPI	HNGS Standard Gamma-Ray
HTHO	PPM	HNGS Formation Thorium Concentration
HURA	PPM	HNGS Formation Uranium Concentration
PEF8	B/E	High Resolution Formation Photoelectric Factor
PEFZ	B/E	Standard Resolution Formation Photoelectric Factor
RD1	IN	Radius 1
RD2	IN	Radius 2

Tab. 3-2: Cont.

Curve/channel	Units	Description
RD3	IN	Radius 3
RD4	IN	Radius 4
RD5	IN	Radius 5
RD6	IN	Radius 6
RHGE_WALK2	G/CC	Matrix Density from Elemental Concentrations (SpectroLith WALK2 Model)
RHO8	G/C3	High Resolution Formation Density
RHOZ	G/C3	Standard Resolution Formation Density
RLA0	OHMM	Apparent Resistivity from Computed Focusing Mode 0
RLA1	OHMM	Apparent Resistivity from Computed Focusing Mode 1
RLA2	OHMM	Apparent Resistivity from Computed Focusing Mode 2
RLA3	OHMM	Apparent Resistivity from Computed Focusing Mode 3
RLA4	OHMM	Apparent Resistivity from Computed Focusing Mode 4
RLA5	OHMM	Apparent Resistivity from Computed Focusing Mode 5
RT_HRLT	OHMM	HRLT True Formation Resistivity
RXO8	OHMM	Invaded Formation Resistivity filtered at 8 inches
RXOZ	OHMM	Invaded Formation Resistivity filtered at 18 inches
RXO_HRLT	OHMM	HRLT Invaded Zone Resistivity
SIGF	CU	Formation Capture Cross Section
SP	MV	Spontaneous Potential
STOF	IN	Effective Standoff in Limestone
SV	MPa	Overburden vertical stress (Sv)
TMP	DEGC	Mud Temperature
U8	B/C3	High Resolution Volumetric Photoelectric Factor
UZ	B/C3	Volumetric Photoelectric Factor
WANH_WALK2*	W/W	Dry Weight Fraction Anhydrite/Gypsum (SpectroLith WALK2 Model)
WCAR_WALK2*	W/W	Dry Weight Fraction Carbonate (SpectroLith WALK2 Model)
WCLA_WALK2*	W/W	Dry Weight Fraction Clay (SpectroLith WALK2 Model)
WCOA_WALK2*	W/W	Dry Weight Fraction Coal (SpectroLith WALK2 Model)
WEVA_WALK2*	W/W	Dry Weight Fraction Salt (SpectroLith WALK2 Model)
WPYR_WALK2*	W/W	Dry Weight Fraction Pyrite (SpectroLith WALK2 Model)
WQFM_WALK2*	KGF/KGF	Dry Weight Fraction Quartz+Feldspar+Mica (QFM) (SpectroLith WALK2 Model)
WSID_WALK2*	W/W	Dry Weight Fraction Siderite (SpectroLith WALK2 Model)

* Qualitative data should only be used as a lithology indicator.

3.3.2 Gaps in log coverage

Optimising the petrophysical log and MHF testing coverage was an objective of the logging and testing campaigns, in particular for the potential Opalinus Clay rock host. Despite best efforts, gaps in log coverage are an inherent limitation in wireline logging operations.

Complete log coverage at changes in drilling section is possible if the acquisition of the lowermost part of the drilling section is repeated later with the acquisition of the uppermost part of the drilling section below. Logs acquired with the same sensor, which overlap over two sections can then be merged providing complete coverage. This is not always possible due to limitations related to tool string geometry, borehole conditions and borehole design. Examples include:

- Cuttings infill the bottom of the hole preventing the tool string from reaching total depth.
- The tool string should not tag the bottom hole with certain fragile tools (e.g. UBI).
- The offset of the sensors relative to the bottom of the tool string
- The length of rathole (length from section bottom to next casing shoe) available for logging in the section below is too short. If the casing shoe is too close to the bottom of the section and the lowermost part of the open hole was not logged before casing installation, some log coverage will be lost.
- The rathole available for logging in the section below is first enlarged, and its diameter is different (e.g. 17 1/2") from that of the cored section below (6 3/8"). Abrupt changes in borehole size are not favorable for logging because they are often associated with bad hole and eccentered tools in contact with the borehole wall acquire logs of degraded quality, causing gaps in log coverage.

The above factors were taken into consideration in the design of work programs. For each logging campaign, project guidelines defined the balance between the optimisation of log coverage (short tool strings, more runs, longer campaign) and saving rig time and associated costs (slightly longer tool strings, less runs, shorter campaign).

For the main drilling sections where petrophysical logs were acquired, a summary of the meterage of logged data and the percentage of total depth this data represents is summarised in Tab. 3-3. Coverage is lost in the Dogger-Lias host rock sequence as a result of operational drilling issues which ultimately resulted in the BUL1-1B sidetrack operation. For example, a significant meterage of invalid data was a consequence of the cement sheath introduced during sidetracking operations which severely affects most of the petrophysical measurements.

Tab. 3-3: Summary of Petrophysical Log Coverage from Drilling Section II to TD

Measurement	**Section 2 to TD**		**Opalinus Clay and Bounding Formations (Dogger-Lias)**	
	Meterage	**Coverage**	**Meterage**	**Coverage**
Total Gamma Ray	829.5	98.9%	225.2	100.0%
Resistivity	760.6	90.7%	169.5	75.2%
Density (PEF)	749.5	89.4%	149.6	66.4%
Neutron	751.2	89.6%	155.9	69.2%
Sonic	738.8	88.1%	154.1	68.4%
Caliper	831.2	99.1%	225.2	100.0%
Spectral Gamma Ray	744.0	88.7%	139.1	61.8%
ECS	725.3	86.5%	147.4	65.4%
FMI (Borehole Image)	795.5	94.9%	181.7	80.7%

The depths at which there were gaps in log coverage in the final composite dataset are detailed in App. A5, Composite log generation.

3.4 Petrophysical logging results and description

The main features of the petrophysical logs of the composite dataset are described below by lithostratigraphic units.

3.4.1 Cenozoic: Quaternary, USM II, USM I and Siderolithikum

The Cenozoic units were logged in a large diameter hole beyond the service provider's stated hole-size specification. Consequently, only the corrected total GR is regarded as a quantitative log. The corrected total GR typically ranges from 27.7 to 75 GAPI, except for a radioactive peak at 112 m MD which reaches up to 255.5 GAPI (Fig. 3-1).

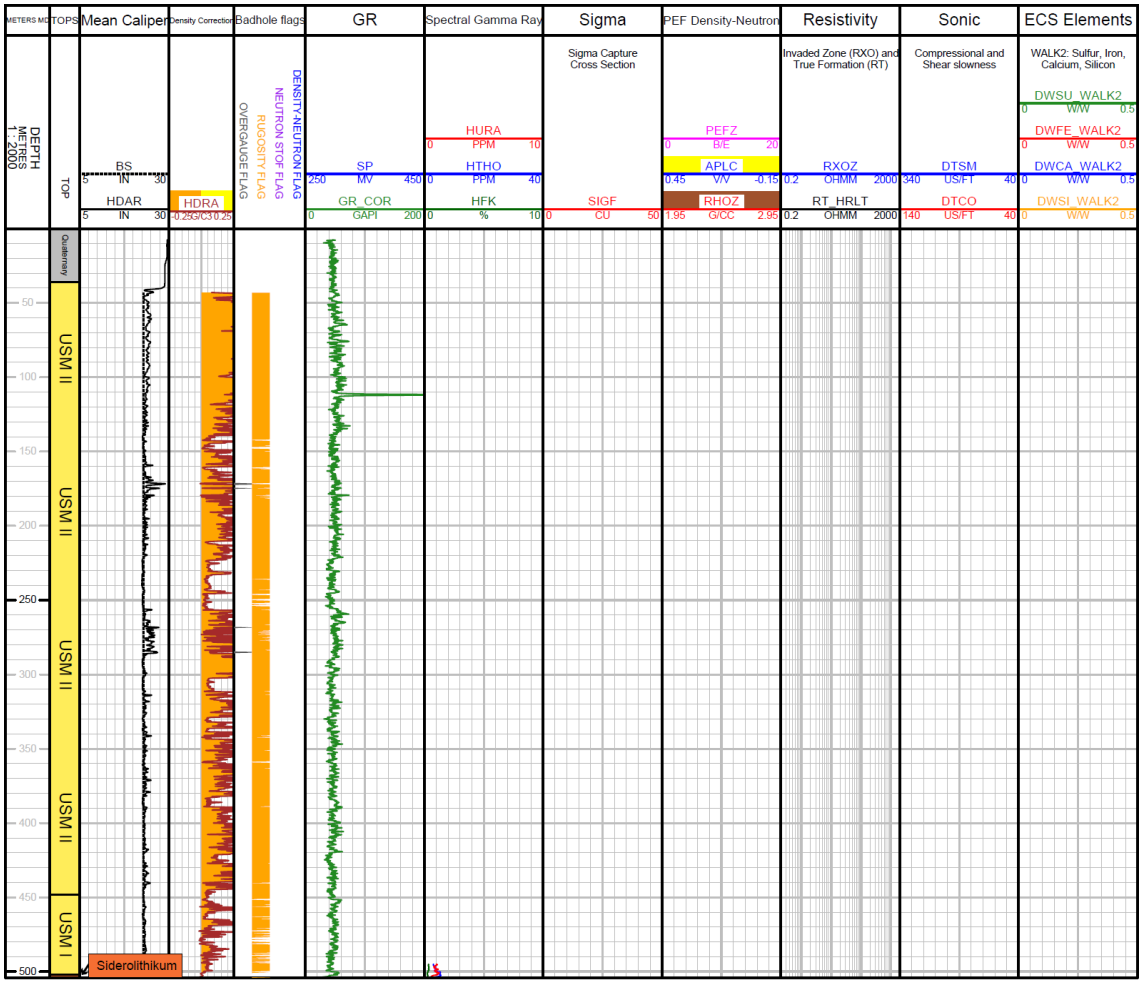

Fig. 3-1: Main logs of the composite dataset in the Cenozoic units

3.4.2 Malm: "Felsenkalke" / "Massenkalk" to Wildegg Formation (504 to 805.38 m MD)

The top of the Malm was not well characterised in the wireline logs because only the corrected total GR (in a large diameter hole) was useable. However, a small drop in total radioactivity is observed at the interface between the Siderolithikum and the Malm.

Except for some short intervals with poor hole conditions, especially in the upper «Felsenkalke» / «Massenkalk», log responses reflect the borehole lithology well (Fig. 3-2). Logs in these formations show:

- Intervals of very low corrected total GR (0 to 24 GAPI) that are often correlated with low neutron (APLC: 0 to 0.10 v/v) and bulk density (RHOZ: 2.71 to 2.50 g/cm^3), which is an almost a perfect overlap with the neutron-density limestone-compatible scale. The compressional sonic DTCO ranges from 49 to 55 µs/ft and the shear sonic DTSM from 300 to 380 µs/ft. These log ranges are consistent with a tight to low porosity, clay-free limestone, with a photoelectric factor PEFZ near the calcite endpoint (5.1 B/E). The sigma (SIGF) endpoint is close to that of calcite at 7.1 CU.
- In several intervals (in particular from 538 to 552 m MD, 655 to 676 m MD, and below 741 m MD), the corrected total GR increases, the density-neutron separation increases and the ECS silicon content picks up (DWSI: up to 0.12 W/W), while the calcium content (DWCA) decreases. The sonic DTCO and DTSM are slower compared to the clean limestone. This demonstrates a progressive increase in clay content, confirmed by an increase in sigma in a calcitic matrix (PEFZ close to 5.1 B/E). The deep resistivity RT_HRLT decreases accordingly. The spectral GR potassium (HFK) and thorium (HTHO) values suggest the presence of illite and non-potassic clay minerals (for instance kaolinite, smectite). The thorium/potassium ratio is commonly used as a qualitative indicator of mineralogical composition. The reader can refer to Serra (1983) about the interpretation of the spectral GR logs in a sedimentary environment, and to the tool manufacturer interpretation charts Lith-1 and Lith-2 for the spectral GR (Schlumberger 2013). Note that this more argillaceous lithology sometimes also affects the borehole quality with significant washouts impacting the log quality.

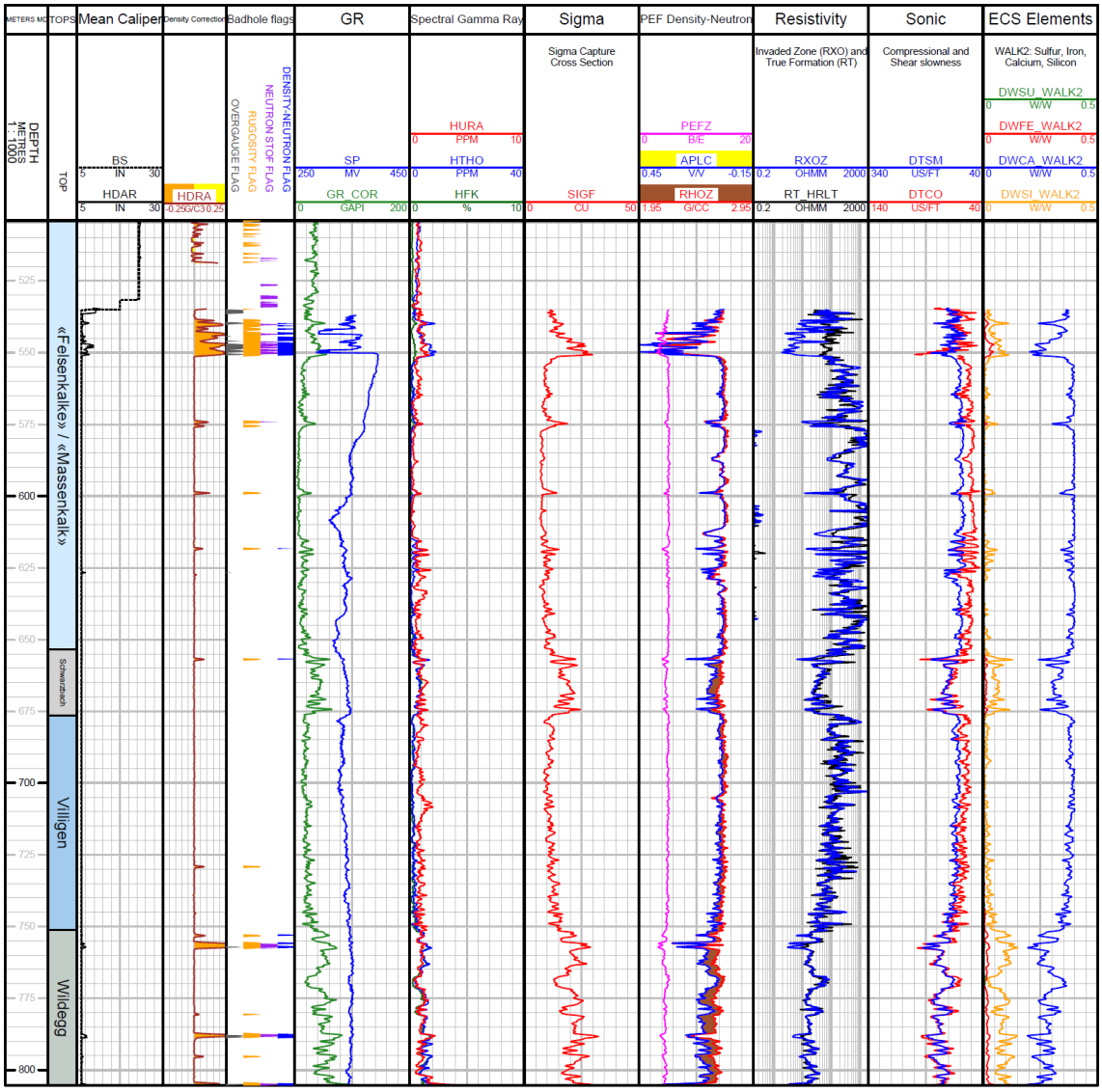

Fig. 3-2: Main logs of the composite dataset in the «Felsenkalke» / «Massenkalk» to Wildegg Formation

3.4.3 Wutach Formation to «Murchisonae-Oolith» unit (805.38 to 891.75 m MD)

The top of the Dogger (Wutach Formation) can be identified by a sharp increase in GR and sigma (SIGF) when entering argillaceous limestones and marls of the Wutach and the Variansmergel Formations (Fig. 3-3). Furthermore, the ECS iron-content (DWFE) increases, which suggests the presence of siderite from the top of the Wutach Formation. Due to the good hole conditions, log responses reflect the borehole lithology well except for a few short intervals with bad hole conditions. Logs in the Wutach Formation to «Murchisonae-Oolith» unit are characterised by:

- Intervals of moderate corrected total GR (11 to 27 GAPI) are often correlated with low neutron (APLC: 0 to 0.10 v/v) and density (RHOZ: 2.71 to 2.60 g/cm^3), which is almost a perfect overlap with a low positive separation in the neutron-density limestone-compatible scale (shaded brown). This suggests an almost clay-free, tight limestone lithology. According to the ECS, the silicon (DWSI) is always above 0 W/W and remains below 0.06 W/W, indicating a weak presence of silica. The PEFZ is in the range of 4.9 to 5.1 B/E, typical for a calcitic matrix with very low clay content. SIGF is slightly too high for pure calcite (close to 9 CU instead of 7.1 CU for pure calcite), likely caused by the small clay volume. The sonic DTCO ranges from 53 to 56 µs/ft, fully consistent with a tight, slightly argillaceous limestone.
- The logs show a gradual transition from the clean limestone response to slightly more radioactive rocks that can be interpreted as argillaceous rocks, with moderate to high clay content (GR_COR: 21 to 121 GAPI) from the base of «Herrenwis» to «Murchisonae-Oolith» units. Borehole conditions were often degraded (see the bad hole flags), affecting the log response and particularly the neutron-density logs (absent density-neutron separation, whereas a more pronounced separation is expected in clay-rich formations). The increase in corrected total GR correlates well to an increase in SIGF and silicon content DWSI, a decrease in calcium content (DWCA) and PEFZ, an increase in the sonic slowness (DTCO) and a decrease in the deep resistivity (RT_HRLT), indicating more argillaceous limestones, marls and shales in the bottom of the interval. The spectral GR potassium (HFK) and thorium (HTHO) curves once again suggest the presence of illite and non-potassic clay minerals (e.g. kaolinite, smectite).

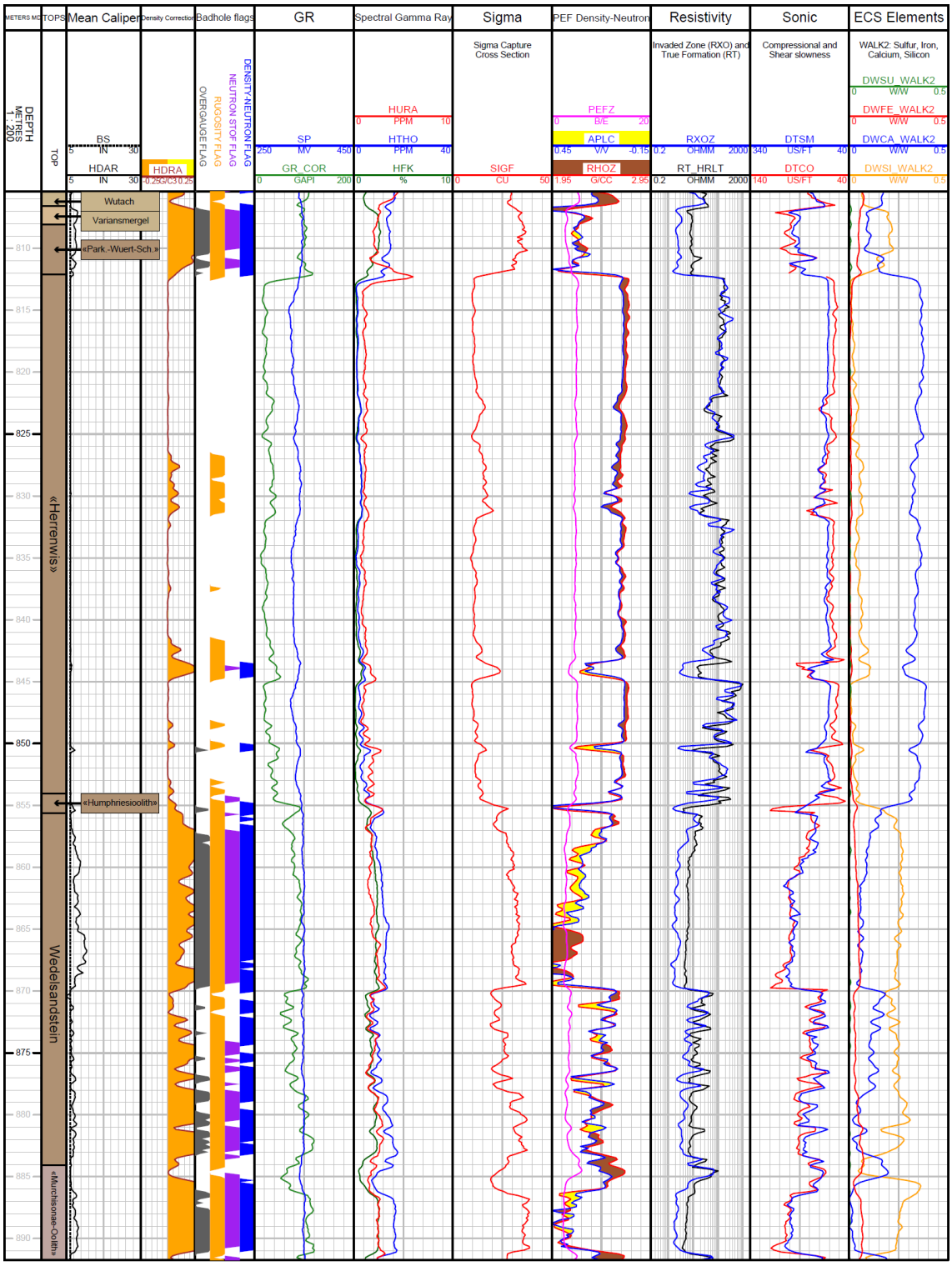

Fig. 3-3: Main logs of the composite dataset in the Wutach Formation to «Murchisonae-Oolith» unit

3.4.4 Opalinus Clay (891.75 to 996.01 m MD)

Due to very adverse borehole conditions (cement sheath in the abandoned nearby borehole before side-tracking), the logs below 938 m MD cannot be used for quantitative analysis. Only the corrected GR was kept in this interval and should only be used in a qualitative manner because its attenuation could not be fully corrected (Fig. 3-4).

In the upper part of the Opalinus Clay (891.75 to 938 m MD), bad hole conditions affected log responses to lithology (bad hole flags in Fig. 3-4). In particular, the neutron-density curves showed little or even inverted separation in several intervals (906 to 912 m MD and below 932 m MD). A larger separation is expected in clay rich formations, for instance as was observed in the interval 891.75 to 900 m MD (brown shading).

In the Opalinus Clay, logs show the following attributes (Fig. 3-4):

- The corrected total GR ranges from 73 to 121 GAPI, thus the formation was interpreted as argillaceous with intermediate to high clay content. Sigma (SIGF) correlates very well (positively) to GR_COR, ranging from 24 to 41 CU. The compressional wave slowness DTCO was high (slow formation) and generally above 90 µs/ft due to high volumes of clay.
- Density (RHOZ) and neutron (APLC) could only be used in hole sections of good quality and show a positive separation confirming the moderate to high clay content.
- The lowest GR_COR readings (73 to 95 GAPI) coincide with a slightly higher deep resistivity (RT_HRLT), increased sonic (DTCO, DTSM) and often high calcium content DWCA, suggesting that these responses were mostly driven by the calcite content.
- The ECS iron-content (DWFE) increases in the Opalinus Clay, showing the presence of iron-rich minerals (siderite, pyrite or chlorites).
- The spectral GR potassium (HFK) and thorium (HTHO) logs suggest the presence of illite and non-potassic clay minerals (e.g. kaolinite, smectite).
- A thin layer at 908 m MD suggests a high PEFZ (5.6 B/E) and high iron-content (DWFE: 0.12 W/W), fast sonic velocities and higher resistivity, indicating a siderite-rich bed.

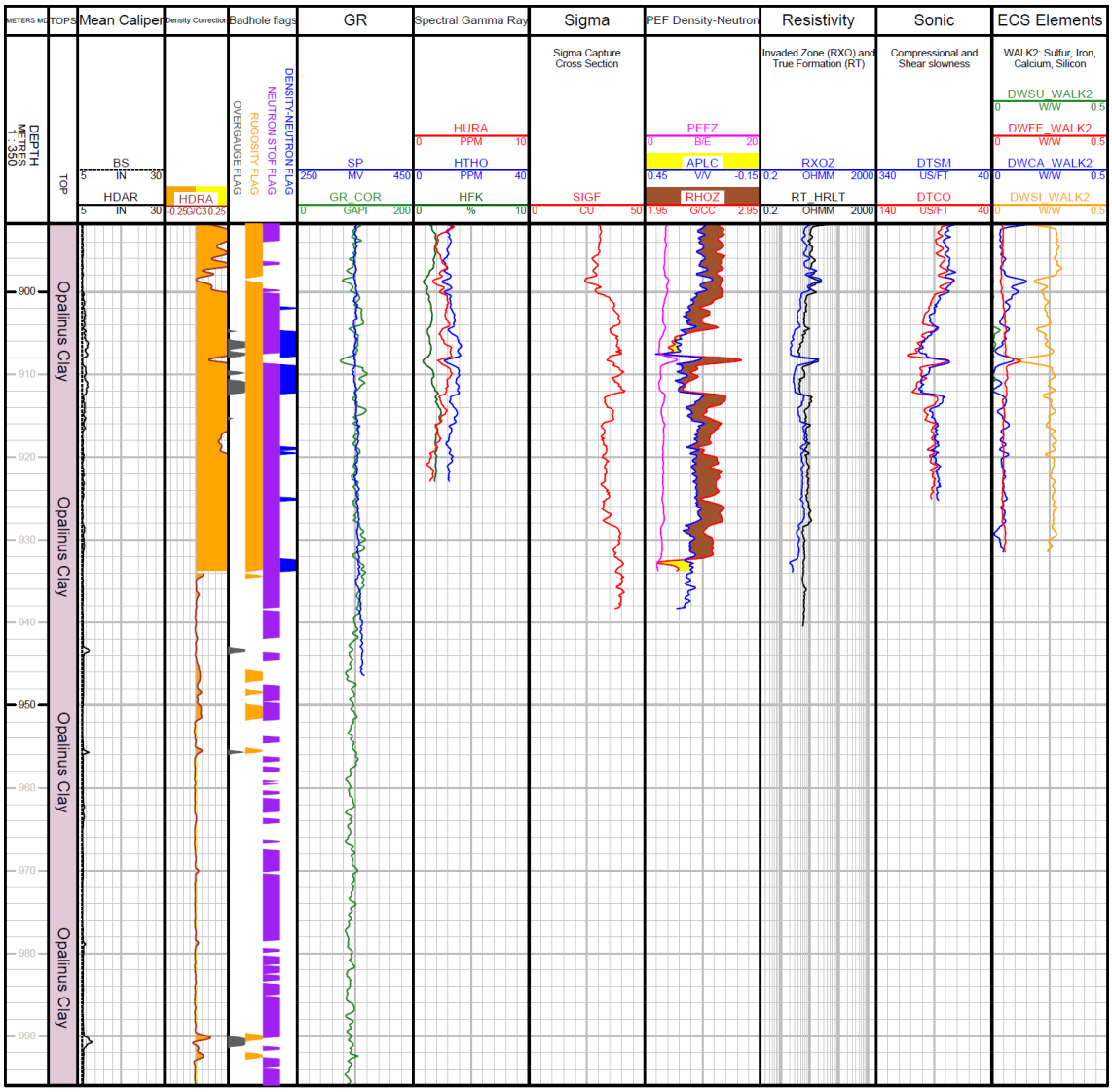

Fig. 3-4: Main logs of the composite dataset in the Opalinus Clay

3.4.5 Staffelegg Formation (996.01 to 1'030.53 m MD)

The transition from the Opalinus Clay to the Staffelegg Formation was difficult to identify based on the wireline log response, because the upper Staffelegg Formation (996 to 1'007 m MD) in the side-track hole was still affected by the nearby cement sheath in the main borehole track. Nevertheless, the top of the Staffelegg Formation seems to correspond with the first sharp decrease in corrected total GR at the formation top (996 m MD).

Below this zone affected by the nearby cement sheath, hole conditions were variable with some degraded intervals as indicated by the bad hole flags (Fig. 3-5). Outside of the bad hole intervals, log responses reflect the borehole lithology. Logs show the following attributes (Fig. 3-5):

- Alternations of high corrected total GR (up to 127 GAPI) and moderate corrected total GR (down to 15 GAPI) indicate the presence of almost clay-free and shaly lithologies. A very radioactive thin event was noticeable at 1'007.5 m MD, likely corresponding to a layer rich in organic matter (GR_COR is up to 249 GAPI)
- Density – neutron logs were mostly affected by bad hole conditions.
- The ECS elemental spectroscopy shows a significant amount of silicon (DWSI) in some layers and calcium (DWCA) in others. Silicates, carbonates, and clays are present in these units in agreement with the description of the cuttings. The multi-mineral interpretation detailed in Dossier X will help to better understand this complex mineralogy.

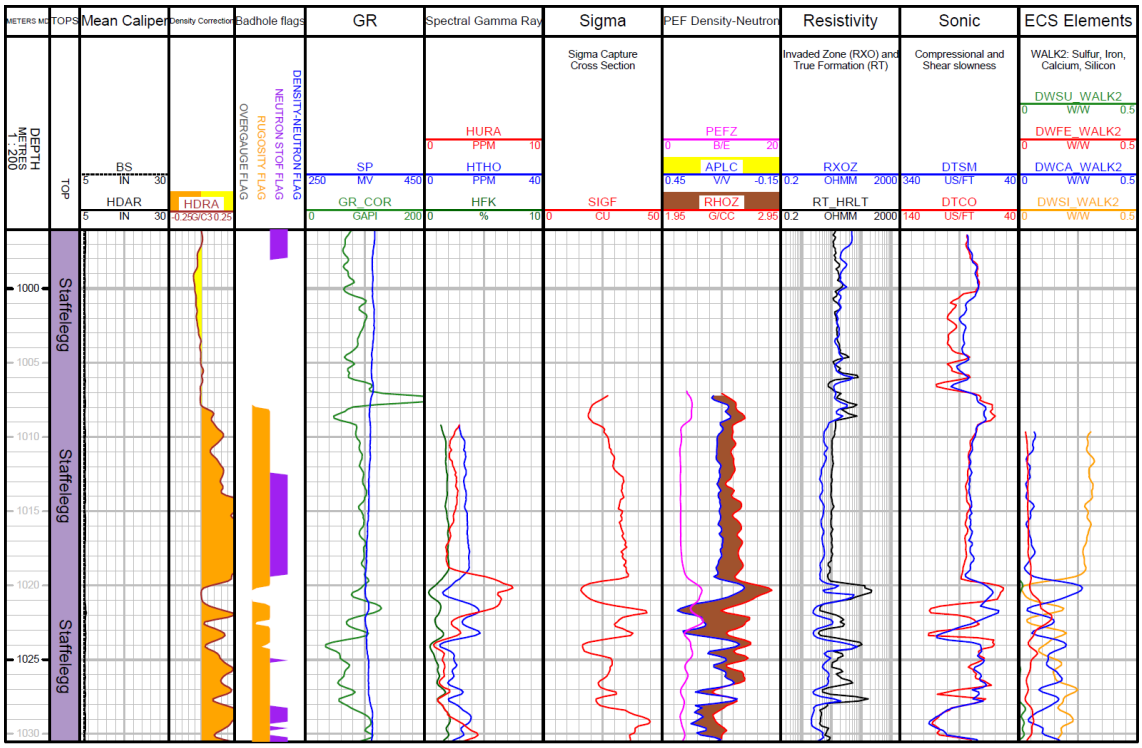

Fig. 3-5: Main logs of the composite dataset in the Staffelegg Formation

3.4.6 Klettgau and Bänkerjoch Formation (1'030.53 to 1'132 m MD)

The Top Triassic (Klettgau Formation) was evident in the wireline logs characterised by decreases in the total corrected GR and sonic slowness DTCO (faster formation) and an increase in ECS calcium content (DWCA). These indicators are consistent with an increase in dolomite content when entering the Triassic.

Hole conditions were degraded in most of this interval as indicated by the bad hole flags (Fig. 3-6). Bad hole conditions affected log responses to lithology, particularly the density and neutron logs. The Klettgau and Bänkerjoch Formations are show the following attributes (Fig. 3-6):

- Density-neutron logs in bad hole intervals could not be used.
- The corrected total GR ranges from low (down to 6 GAPI in the lower Bänkerjoch Formation) to high (up to 167 GAPI in the lower Klettgau Formation), indicating clay-free and shaly units.
- The ECS Sulphur concentration (DWSU) and the density-neutron response (APLC-RHOZ) suggests a significant presence of anhydrite-rich layers (particularly in the Bänkerjoch Formation), which was confirmed by the description of the cuttings. The ECS calcium content ranges from almost 0 W/W to more than 0.36 W/W, suggesting the presence of carbonates in variable amounts.

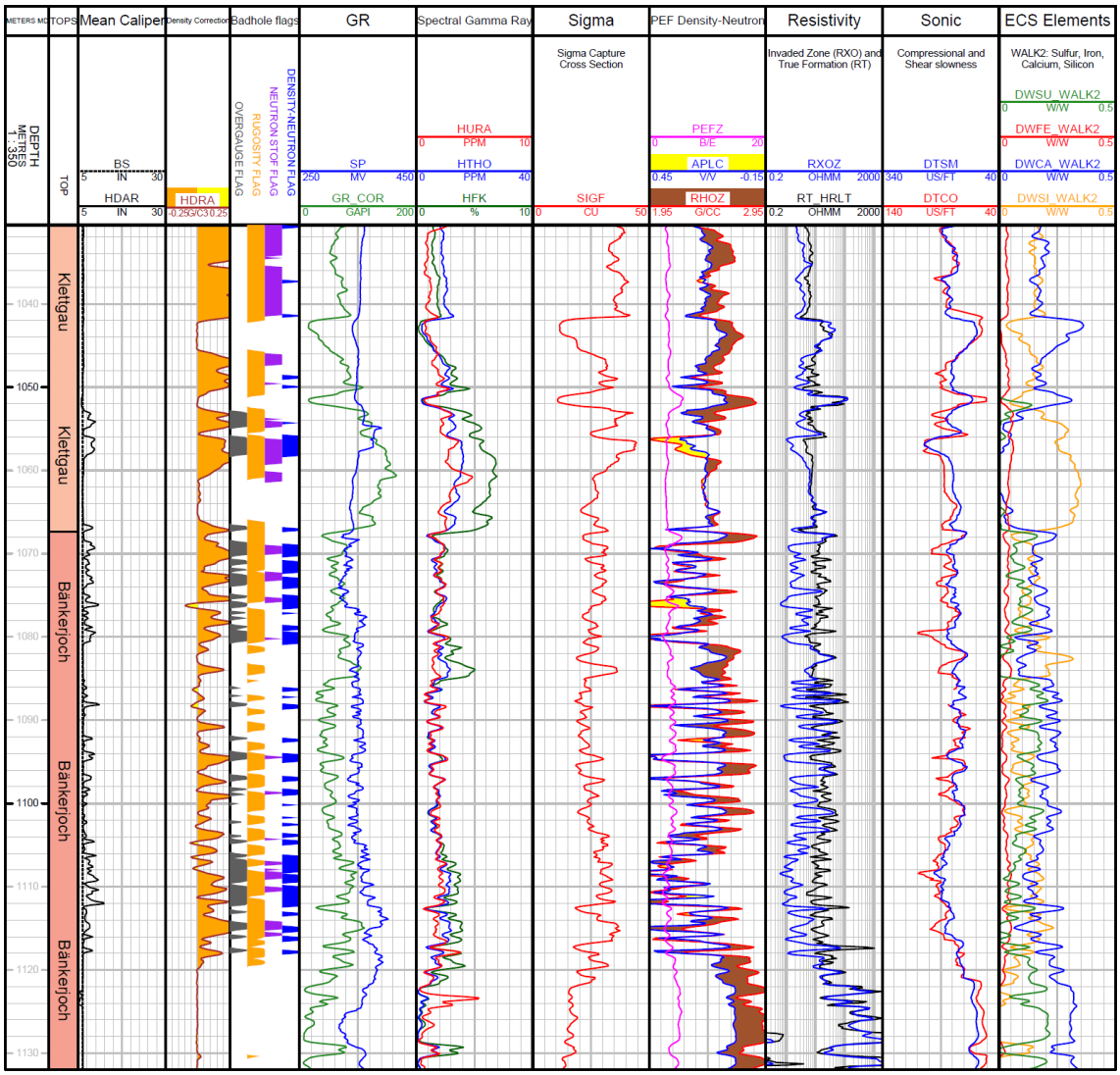

Fig. 3-6: Main logs of the composite dataset in the Klettgau and Bänkerjoch Formations

3.4.7 Schinznach Formation (1'132 to 1'204.58 m MD)

The top of the Schinznach Formation is identified by the disappearance of the ECS Sulphur content (DWSU) below the lowest anhydrite bed of the Bänkerjoch Formation.

Due to the good hole conditions, log responses reflect the borehole lithology well and are characterised by the following attributes (Fig. 3-7):

- The overall low to moderate corrected total GR (10 to 50 GAPI) indicates a low clay content. A high GR peak (197 GAPI) is visible at 1'135.1 m MD, which coincides with high ECS silicon content DWSI (0.29 W/W) and no calcium (DWCA) at that depth, indicating a thin shale bed.
- The ECS calcium concentration was high, ranging from 0.3 from 0.4 W/W, indicating that high amounts of carbonates are present (dolomite based on PEFZ log, see below).
- The positive density-neutron separation (RHOZ-APLC; shaded brown in Fig. 3-7) and the PEFZ values (close to 3.1 B/E) suggest a lithology dominated by dolomite down to 1'174.5 m MD.
- Below 1'174.5 m MD the density-neutron separation reduces and PEFZ values shift to higher values, which indicates dolomitic limestones. This was confirmed by the description of the cuttings.
- Sigma (SIGF) readings were generally in agreement with the presence of carbonates (7 to 13 CU), except in a shale bed at 1'135.1 m MD (where SIGF was above 30 CU).

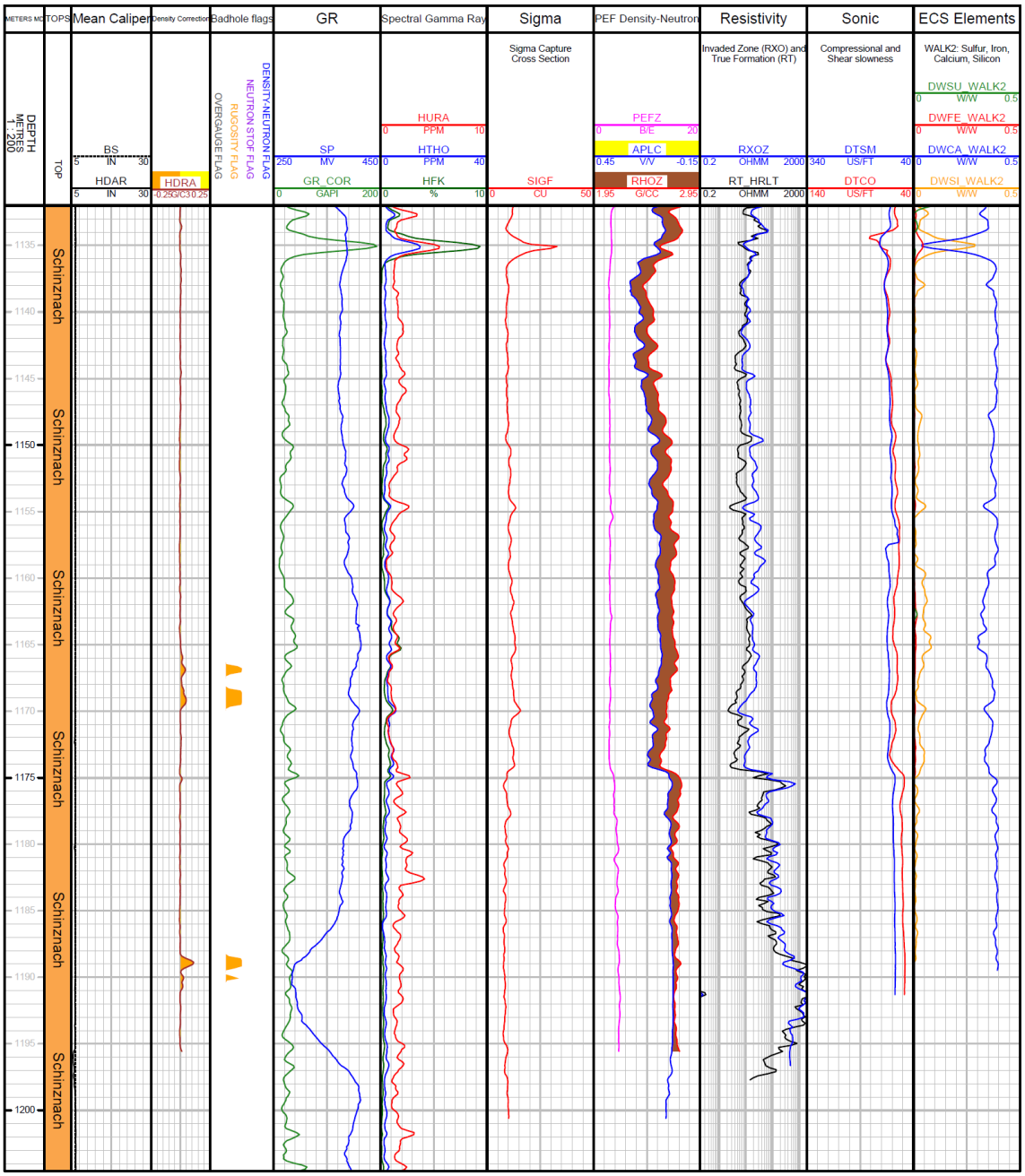

Fig. 3-7: Main logs of the composite dataset in the Schinznach Formation

3.4.8 Zeglingen Formation (1'204.58 to 1'267.94 m MD)

The top of the Zeglingen Formation could not be identified in wireline logs because it was above the 9 5/8" casing shoe at 1'205 m MD. Due to the good hole conditions, log responses reflect the borehole lithology well except in the rathole interval between 1'205 and 1'210 m MD (Fig. 3-8). Logs were show the following attributes:

- Low to moderate corrected total GR ranging from 3 to 96 GAPI, which indicates clay-free to intermediate clay contents.
- The neutron APLC is not valid in the rathole (1'205 to 1'210 m MD) owing to the high standoff of the tool (STOF; intervals of bad hole flagged in purple and blue).
- The main lithologies can be inferred from the ECS elemental concentrations (Si, Ca, Fe, S): high calcium DWCA in the carbonate beds (dolomite and calcite) and high sulfur DWSU in the anhydrite layers where density readings were equal to or higher than 2.95 g/cm^3.
- The salt interval between 1'245 and 1'260 m MD is well characterised in the density-neutron separation (crossover, shaded yellow in Fig. 3-8), the sonic compressional slowness (close to 67 µs/ft) and the very resistive response of the HRLT logs (RT_HRLT saturated at 100'000 Ohm.m). The salt was, however, not visible in the SIGF measurements (theoretical value for halite: 754 CU)
- A dolomitic porous interval is visible from 1'214 to 1'221 m MD, which was well characterised by the PEFZ value (close to the dolomitic endpoint of 3 B/E).

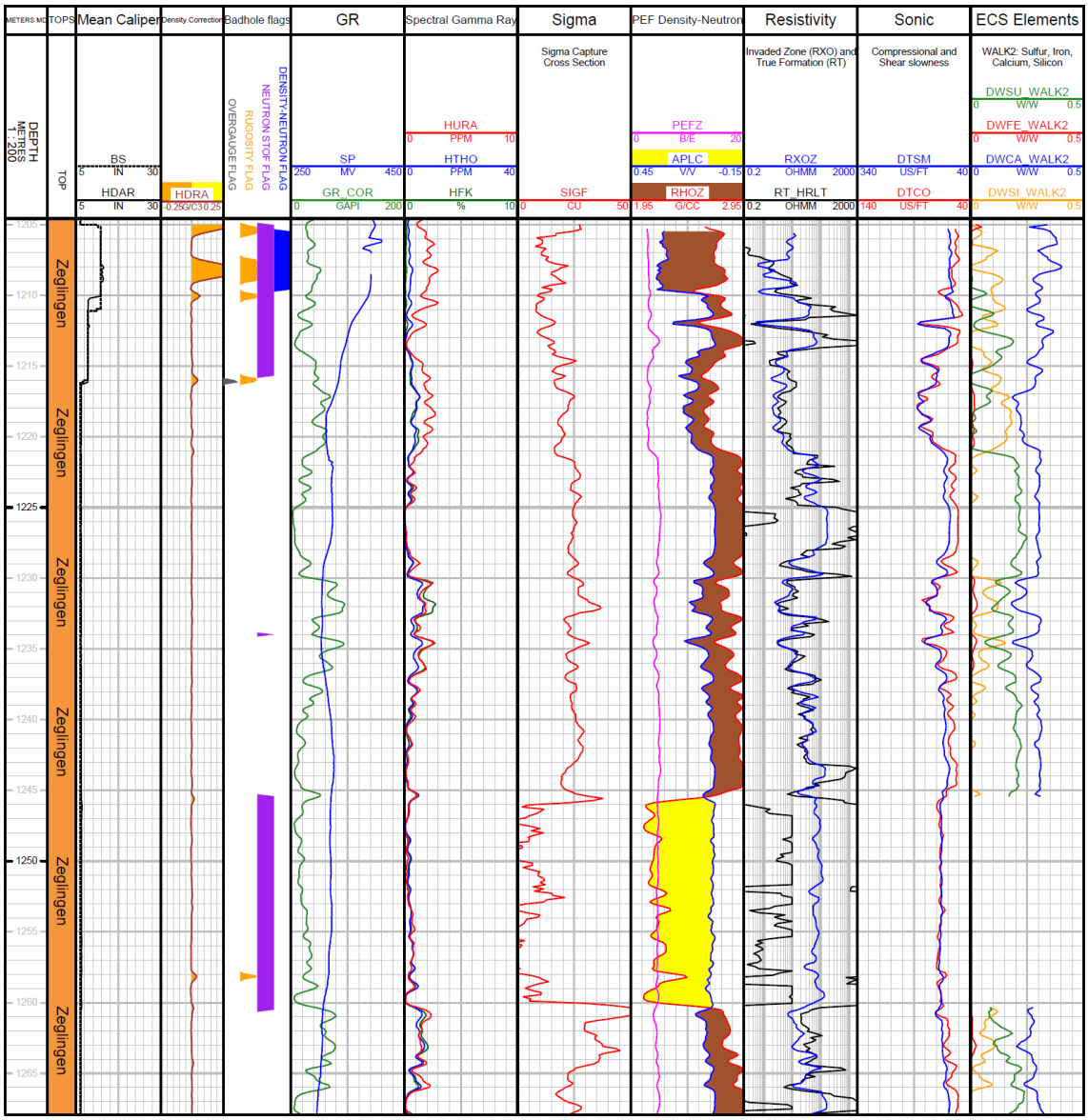

Fig. 3-8: Main logs of the composite dataset in the Zeglingen Formation

3.4.9 Kaiseraugst Formation (1'267.94 to 1'306.11 m MD)

The top of the Kaiseraugst Formation is difficult to identify because the wireline logs show no clear transition in the log attributes. Due to the good hole conditions, log responses reflect the borehole lithology well (Fig. 3-9). Logs show the following attributes:

- A high corrected total GR ranging from 9 to 178 GAPI, except in the anhydrite layer (1'275.5 to 1'276.3 m MD) indicating high clay content.
- The density-neutron separation, low resistivity (R_HRLT) and high sigma (SIGF) are consistent with this high GR.
- The ECS element concentrations show high silicon (DWSI) from clastic mineralogy (clay, quartz) and high calcium (DWCA) from dispersed calcite.
- At the base of this formation, the lower SIGF and reduced density-neutron separation indicates an almost clay-free layer from 1'303.5 to 1'305 m MD.

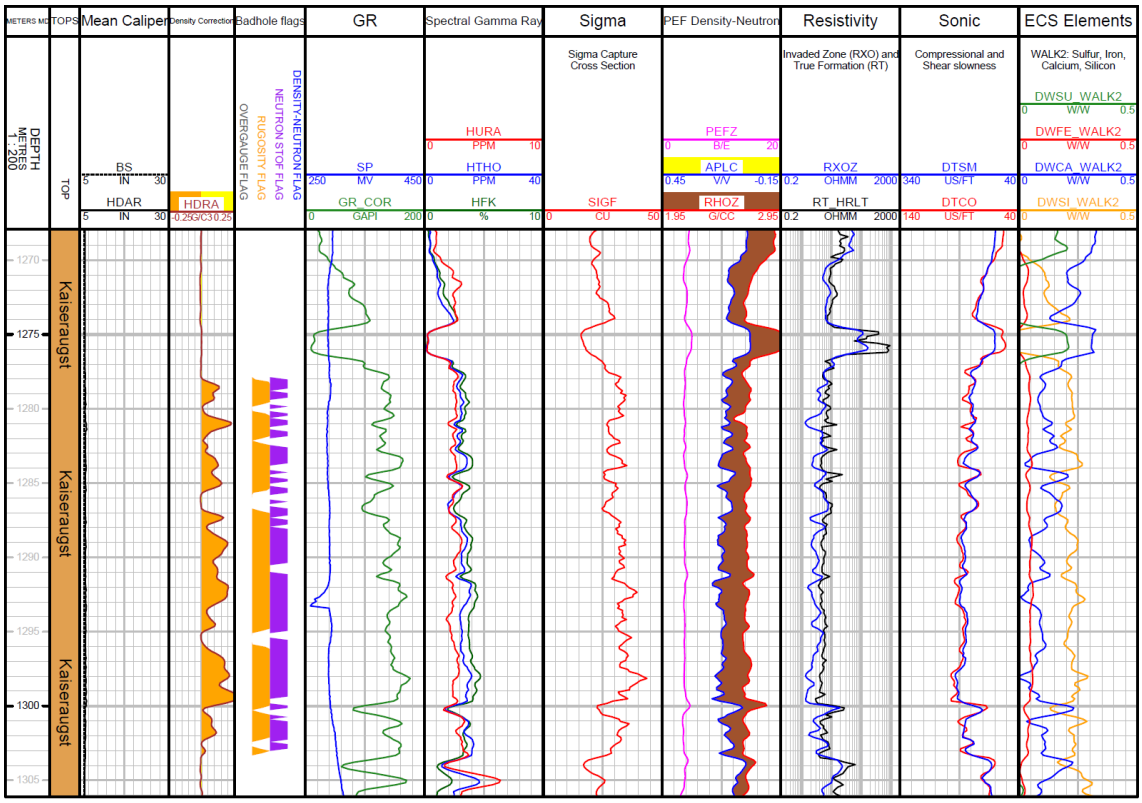

Fig. 3-9: Main logs of the composite dataset in the Kaiseraugst Formation

3.4.10 Dinkelberg Formation (1'306.11 to 1'319.46 m MD)

The top of the Dinkelberg Formation corresponds to a transition from marls to sandstones, which is represented in the logs by an increase in the ECS silicon content (DWSI) and a decrease in calcium (DWCA), as well with a change in the bulk density-neutron separation, where the density log was to the left of the neutron log («crossover» in a limestone-compatible scale, shaded yellow).

Logs respond well to lithology in this formation because hole conditions were good (Fig. 3-10) and are characterised by the following attributes:

- Logs often show a high corrected total GR ranging from 42 to 145 GAPI. This is typical for siltstones and sandstones that contain radioactive minerals such as K-feldspar and mica (and will be better quantified by the core-calibrated stochastic, multimineral analysis described in Dossier X).
- The slight inverse neutron-density separation indicates the presence of quartz minerals (and/or feldspars), as shown with the yellow shading in Fig. 3-10.
- The ECS element concentrations show high silicon (DWSI) from clastic mineralogy (quartz, possibly feldspars). The possible presence of K-feldspars or other radioactive minerals is suggested by comparison of the spectral GR concentrations of potassium (HFK), thorium (HTHO) and uranium (HURA).

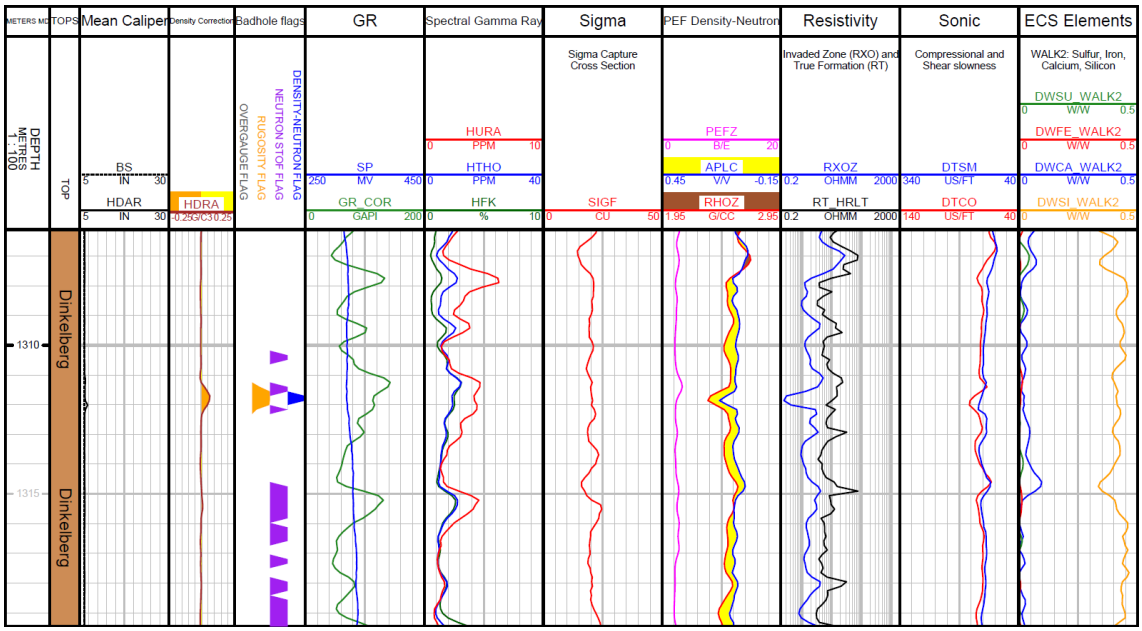

Fig. 3-10: Main logs of the composite dataset in the Dinkelberg Formation

3.4.11 Weitenau Formation (1'319.46 m MD to borehole bottom)

The top of the Weitenau Formation is characterised by sharp increases in the corrected total GR (with a strong potassic component HFK) and sigma.

Logs respond well to lithology in this formation because hole conditions were very good (Fig. 3-11). Logs show the following attributes:

- A high total GR, ranging from 109 to 274 GAPI. This is typical for siltstones and sandstones that contain radioactive minerals such as K-feldspar and mica.
- The slightly inversed neutron-density separation indicates the presence of quartz minerals (and/or feldspars) as shown with the yellow shading in Fig. 3-11. This is also supported by the high ECS silicon content (DWSI).
- A very radioactive layer is identifiable at the top of the Weitenau Formation (1'322 to 1'326 m MD), where corrected total GR values increase up to 274 GAPI with high uranium contributions.
- The ECS element concentrations show high DWSI from clastic mineralogy (quartz, possibly feldspars). The potassium (HFK), thorium (HTHO) and uranium (HURA) concentrations suggest the presence of potassic feldspars or other radioactive minerals.

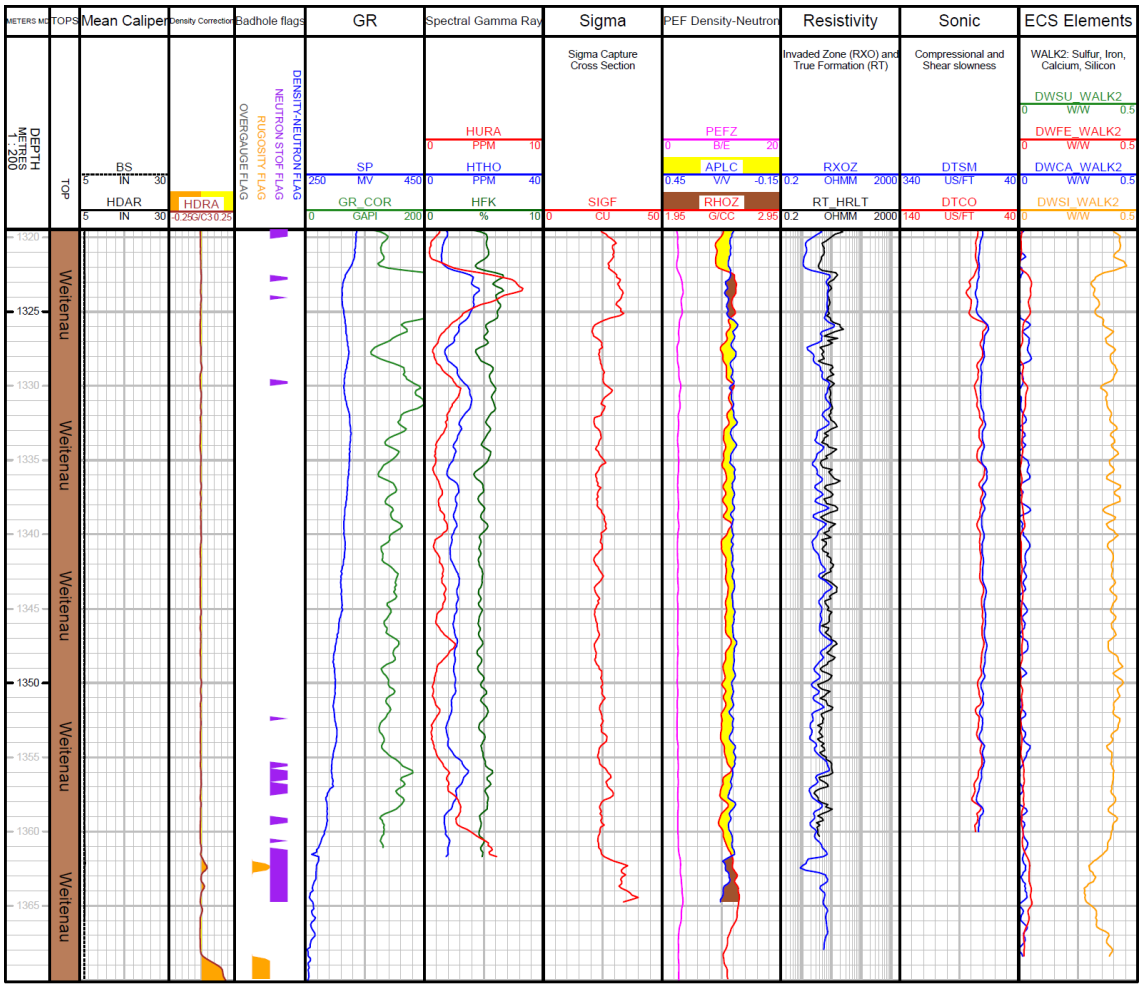

Fig. 3-11: Main logs of the composite dataset in the Weitenau Formation

3.5 Post completion mud temperature

Three temperature re-logs were performed by Schlumberger post completion (in cased hole) on 3-Jun-2020 (Run 5.2.1), 15.12.2020 (Run 5.3.1) and 20.03.2021 (Run 5.4.1) to measure the temperature of the mud after the last mud circulation on 26th November 2019 (see Tab. 2-2). Temperature was measured using the EMS tool, which has an accuracy of ± 1 °C and resolution of 0.1 °C. In Fig. 3-12, only the downlog from Run 5.4.1 is plotted as it is believed to be the most representative of the formation temperature. It was acquired at a slow rate of 275 m/hr to avoid mixing of the hydrostatic mud column. Maximum temperature of 58.30 °C was recorded at 1'179.6 m MD, minimum of 2.15 °C at surface. In Opalinus Clay, temperature is 41.03 – 49.52 °C, and the average geothermal gradient $\Delta T/\Delta D$ = 0.073 °C/m. The overall temperature gradient is higher in the clay-rich units of the Dogger compared to the calcareous units of Malm and Muschelkalk.

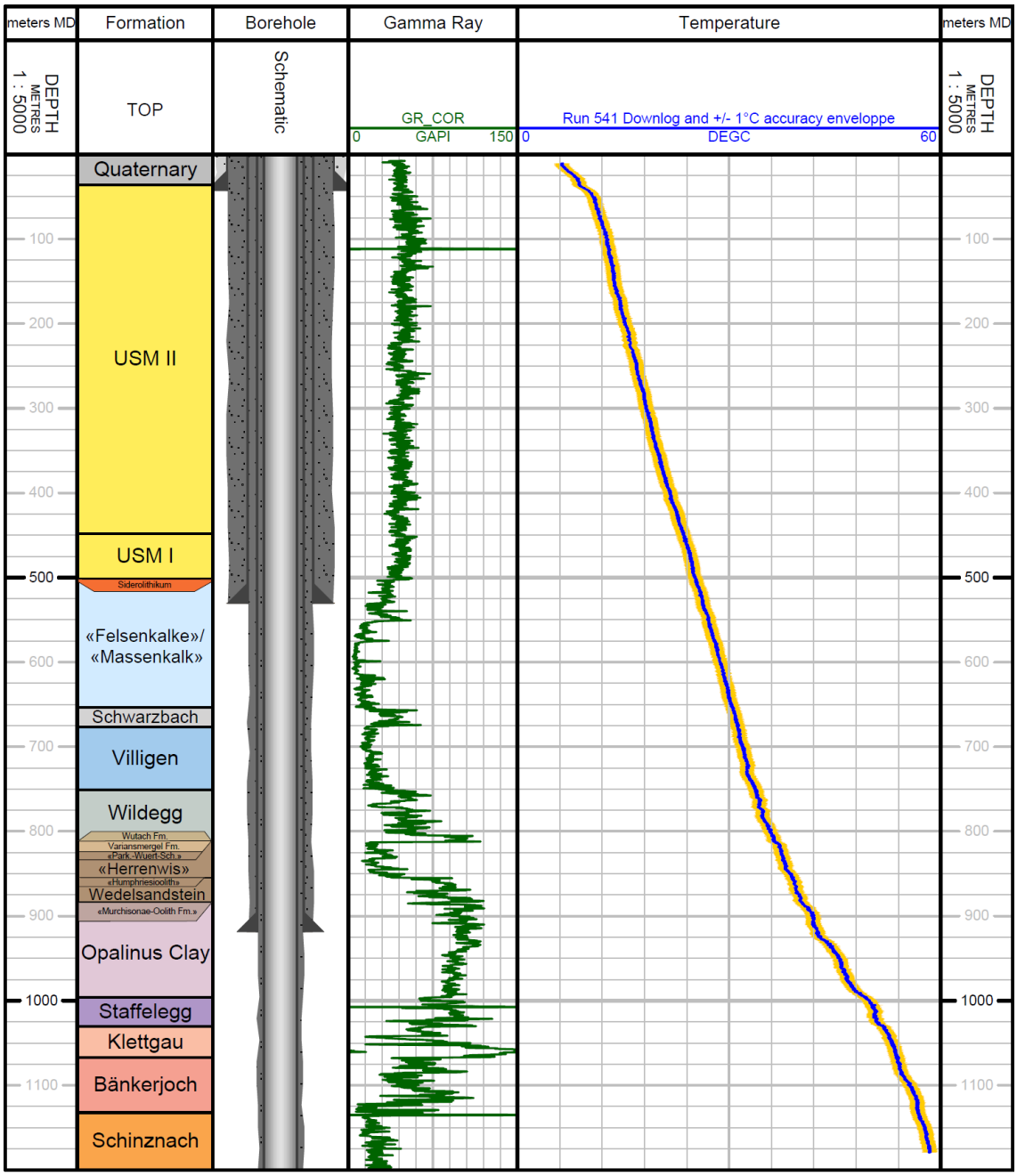

Fig. 3-12: Post-completion temperature log from the downlog pass of Run 5.4.1 (20.03.2021)

A ± 1 °C accuracy enveloppe is drawn in orange around the temperature log

4 Borehole imagery (BHI)

Borehole imaging tools produce high resolution circumferential images of the borehole wall by measuring either resistivity with tool pad contact or ultrasonic velocity. For the BUL1-1 borehole, SLB's Fullbore Formation MicroImager (FMI) and Ultrasonic Borehole Imager (UBI) were used. The FMI comprises of four pads that measure the formation resistivity via an array of buttons (24 per pad) that are pressed against the borehole wall, providing a vertical resolution of 2.5 mm and approximately 90% coverage. The UBI has a rotating sub that sends out acoustic pulses to the formation and measures the amplitude and travel time of the returning signals, providing 5 mm vertical resolution and 100% borehole coverage. In general fractures, faults and bedding are more easily identifiable using the FMI than the UBI as the microresistivity images provide better contrast. However, borehole wall features can be missed if they are located in an area not covered by the tool pad, which is why FMI and UBI images should be used together for image interpretation. In addition, breakouts are typically poorly resolved on microresistivity images because fracturing and spalling associated with these breakouts results in poor contact of the tool pads with the borehole wall.

BHI was used to:

- identify and characterise geological, sedimentological and structural features including bedding, fault planes/zones and fractures
- identify stress-induced borehole phenomena such as tensile drilling-induced fractures and breakouts
- core goniometry
- select MHF testing locations (referred to as Stations herein)
- detect and orient fractures induced by MHF stress measurements

For details on the first three uses of BHI please refer to Dossier V – Structural Geology. Only the latter two will be discussed further in this Dossier.

The BHI that was acquired pre-MHF was quality controlled (QCed), processed and interpreted by GPCI or NiMBUC in a limited amount of time (i.e., rush processing and basic quicklook interpretation). The aim of this quicklook interpretation was to provide a general and quick picture of existing borehole/rock heterogeneities (breakouts, natural and induced fractures, etc.) for the selection of MHF stations immediately after BHI log acquisition and prior to MHF testing. In Fig. 4-1, the workflow used by GPCI and NiMBUC is described. Final processed and spliced pre-MHF image logs are included in the composite plots (Appendices B and C), along with the petrophysical logs and core photographs.

The post-MHF imagery underwent a similar workflow to the pre-MHF imagery, however, only the intervals that underwent stress testing were interpreted. These will be detailed in a future MHF interpretation report. To determine whether fractures were generated or enhanced (opened further) the pre- and post-MHF imagery was plotted side-by-side, along with the MHF test interval and packer positions (see Appendix D).

Step 1: Image QC	
Depth matching	Correlate high resolution image with reference GR
Caliper check	Verify calibration with casing ID, identify if borehole conditions could affect image quality (washouts, mud cake, etc.)
Hardware check	Identify if downhole equipment performance indicators such as gain and voltage supply are consistent
Orientation check	Ensure orientation data are in agreement with borehole azimuth and deviation from independent survey.
Accelerometer check	Accelerometer measurement should be consistent with earth's gravity (1 g = 9.81 +/- 0.03 m/s^2).
Magnetometer check	Magnetometer consistent with theoretical magnetic field strength at location, X-Y magnetometers behave complementary, QC magnetic declination parameters input
Tool movement check	Identification of any stick and pull events using tension and accelerometer measurements
Acquisition check	Verify frame time and cable speed control
Borehole image check	Identification of dead buttons or pads and any casing interference

↓

Step 2: Image processing	
Basic image generation	Azimuthal orientation of images to true or grid north
	Merging of individual tool run passes
	Splicing of data between drilling sections
	If required, invert images to ensure s per industry standards that low value = low resistivity and high value = high resistivity
	If required, correct offsets between pad images
	Bad button detection and correction
Image equalisation and normalisation	Static normalisation involving selecting the normalisation distribution (uniform/Gaussian), equalisation strength, high/low cut-offs for equalisation, etc.
	Dynamic normalisation to enhance local contrasts highlighting features in a selected sliding window of a few metres

↓

Step 3: Basic interpretation	
Manuel picking of features directly from the processed image in accordance with Nagra classification scheme detailed here	Drilling-induced fractures
	Borehole breakouts
	Bedding
	Fractures (conductive, partially conductive, resistive, partially resistive, faint trace)
	Faults (conductive, partially conductive, resistive, partially resistive, faint)

Fig. 4-1: Borehole image processing workflow

5 Micro-Hydraulic Fracturing (MHF)

5.1 Introduction and objectives

A series of stress measurements were performed in the BUL1-1 borehole using the micro-hydraulic fracturing (MHF) technique. MHF testing in boreholes is the only direct method available for measuring rock stress magnitude at great depth. An overview of the methodology can be found in Haimson (1993), Desroches & Kurkjian (1999) and Haimson & Cornet (2003) and references therein. The objectives of the testing program are to acquire data to:

- provide estimates of the in-situ stress state in the Opalinus Clay and adjacent rock formations and
- provide calibration points for mechanical earth models (MEM) of the rock mass (1D, 3D). See Bérard & Prioul (2016) for an overview of mechanical earth models and Plumb et al. (2000) for a definition of an MEM.

Key features include:

- Core images and BHI (FMI and UBI) were used to select the appropriate test depths closest to where geomechanical lab test samples were taken.
- The MHF protocol that was used was tailored in real-time to bracket the far-field closure stress as closely as possible.
- Post-MHF imaging logs were run to determine the trace of the newly created fractures, enabling better allocation of the MHF closure stress to a principal stress direction.
- Sleeve fracturing was regularly used to focus the test on the desired interval; sleeve reopening was used to estimate the maximum horizontal stress when the MHF tests yielded an estimate of the minimum horizontal stress.

5.2 MHF Theory

MHF tests an interval of approximately 1 m, which is sealed above and below by packers that are approximately 0.5 m in length (exact dimensions are dependent on the configuration of the tool string). A schematic showing the successive steps taken for a typical MHF test is presented in Fig. 5-1. Once the interval is sealed, a micro-hydraulic fracturing cycle begins with pressurising the interval (1st step) until fracture initiation. Fluid keeps being injected to extend the micro-hydraulic fracture into the formation by a couple of decimeters (2nd step). Injection is then stopped to allow fracture closure and pressure fall-off is observed (3rd step). Similar steps are repeated, to further extend a refine the testing of the micro-hydraulic fracture until the test is deemed satisfactory.

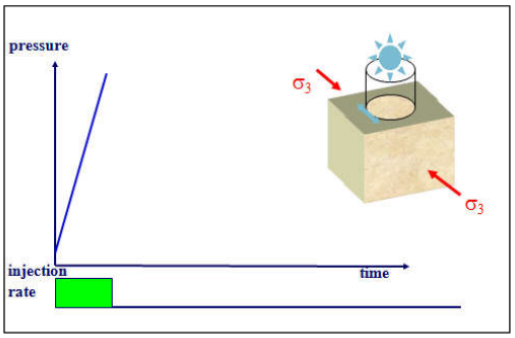

1st step: pressurisation

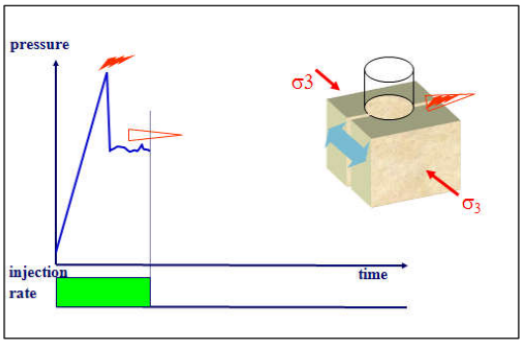

2nd step: fracture propagation

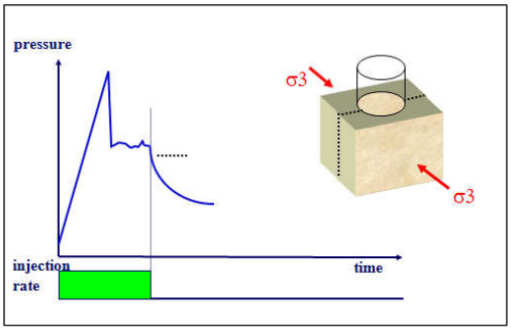

3rd step: Fracture closure

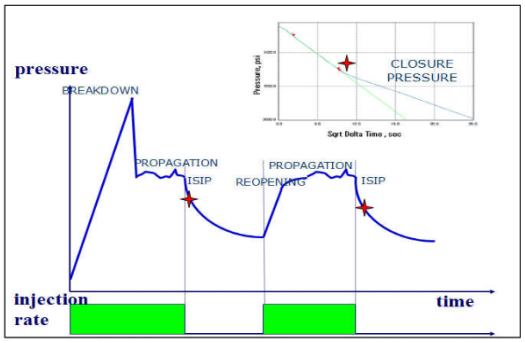

Repeat steps for subsequent cycle(s)

Fig. 5-1: Schematic showing the response of the interval pressure to fluid injection in the interval as a function of time during an MHF test, and associated formation response

5.3 Test protocol

Each test consisted of a succession of steps according to the general test procedure described in Desroches & Kurkjian (1999), Haimson & Cornet (2003) and Wileveau et al. (2007). Although a general procedure was followed for each test, the steps were tailored in real-time to ensure that the pressure records provided the best possible estimate for closure stress. As a result, the number of steps and their nature varied from test to test.

The steps undertaken during a stress test were as follows:

- Depth correlation: validate the cable depth by comparing GR logs with the reference GR log of the borehole.
- Sleeve fracturing: this step is analogous to sleeve reopening (see below) but performed prior to the microhydraulic fracturing operation. The single packer is placed in front of the desired depth and applies pressure to focus the initiation of a longitudinal fracture at the desired interval.
- Packer inflation and leak-off test: the straddle packer is positioned so that the centre of the interval is in front of the desired depth. Packers are inflated to a differential pressure of 300 to 500 psi and the integrity of the seal is observed. The integrity of the seal is further validated by a short injection into the interval.

- Breakdown cycle (steps 1 to 3 in Fig. 5-1): the first cycle in a test during which a hydraulic fracture is propagated was counted as a breakdown cycle (even if technically there is no breakdown, e.g. because a pre-existing drilling-induced fracture was tested). To ensure that cycles are not counted more than once, there was only one breakdown cycle per test. Whether it starts with a step-rate test or ends with a slamback/rebound test (see below), it is still only counted as one breakdown cycle.
- Reopening cycle: any subsequent injection/shut-in cycle during which a fracture is propagated and that neither starts with a step-rate test nor ends with a slamback/rebound test (see below) is counted as a reopening cycle.
- Slamback/rebound test: at the end of an injection cycle during which a fracture was propagated (but not for the first time), the interval is quickly opened and closed for a fast depressurisation and pressure rebounds from a value close to borehole hydrostatic pressure. The slamback occurs immediately after the injection stopped and the rebound is observed until a plateau is reached. If the injection cycle starts with a step-rate test, it is only counted as a step-rate test and not as a slamback/rebound test.
- Step-rate test: an injection cycle during which the rate was increased (or decreased) in steps with at least three different flow rates during the cycle is called a step-rate test. An injection cycle during which the rate was only changed once cannot be counted as a step-rate test because it does not allow a step-rate interpretation.
- Sleeve reopening: the single packer is moved in front of the previously tested interval and pressure is applied with the aim of detecting and reopening the fracture created during the microhydraulic fracturing cycles.

In Fig. 5-2, an example of the pressure record for a MHF test performed in the BUL1-1 borehole is presented (Station 3-2, Run 5.1.8). The top plot (Fig. 5-2a) shows the pressure in the interval, the middle plot (Fig. 5-2b) the fluid injection rate as a function of time and the bottom plot (Fig. 5-2c), also called a reconciliation plot, the characteristic pressures estimated for all cycles for which a fracture was created/tested. For this test, there were a total of 6 cycles, labeled 2 to 7. Cycle 1 is not analysed as it corresponds to the packer inflation and leak off test. Cycle 2 corresponds to the breakdown and propagation cycle, similar to what was depicted in the theory schematic (Fig. 5-1). Cycles 2, 3 and 7 are reopening tests, cycles 4 and 6 are step-rate tests. A slamback/rebound test was performed at the end of cycles 3, 4 and 6. The characteristic pressures presented in the bottom plot reflect the stress acting on the fracture: they validate the creation of a hydraulic fracture and show a clear trend towards convergence that supports that an estimate of the far-field stress can be obtained from the test.

The raw MHF pressure-time and reconciliation plots for all tests conducted in the BUL1-1 borehole are included in Appendix E. In Tab. 5-1, a summary steps taken for each MHF station is given, along with the associated formation/unit that was tested. Stations are presented in operational order.

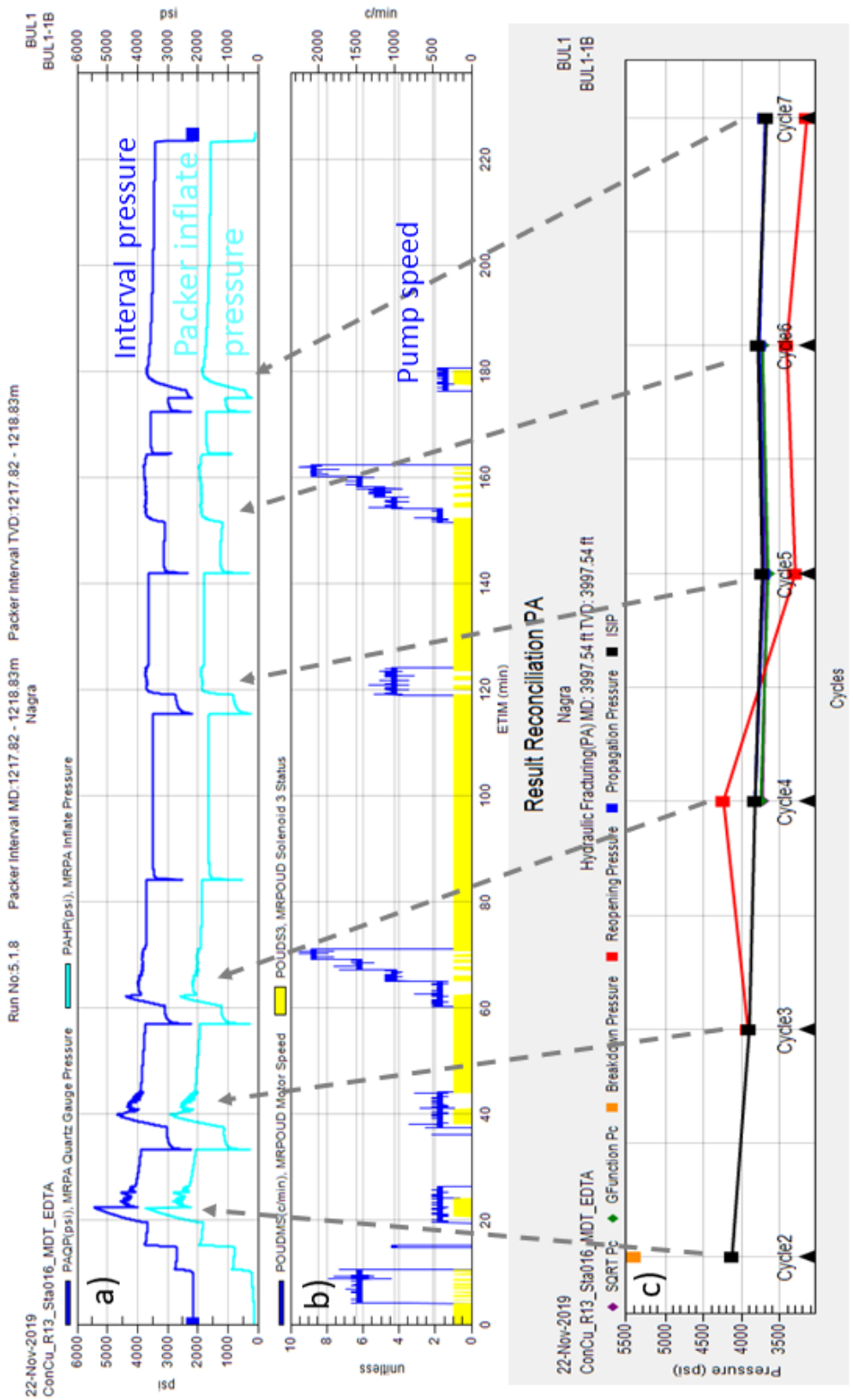

Fig. 5-2: Example of pressure record for MHF test from BUL (Station 3-2, Run 5.1.8)
Pc stands for closure pressure, ISIP stands for Instantaneous Shut-in Pressure.

Tab. 5-1: Summary of MHF station locations and operations carried out for each phase of the BUL1-1B borehole

Phase/ section	**Station**	**Formation/unit**	**Middle interval depth** (m)	**Sleeve fracturing cycles**	**Breakdown cycles**	**Re-opening cycles**	**Slamback/ rebound tests**	**Step-rate tests**	**Sleeve reopening cycles**
2 (Run 2.6.2)	1	Wildegg Fm.	765.25	2	0	0	0	0	No
	2	Wildegg Fm.	772.4	2	0	0	0	0	No
	3	«Herrenwis Unit»	847.1	2	1	3	1	1	2
	4	Wedelsandstein Fm.	871.2	No	0	0	0	0	No
	5	«Herrenwis Unit»	814.4	No	1	4	2	0	2
	6	Schwarzbach Fm.	668.4	2	1	2	1	1	2
	7	«Felsenkalke»/ «Massenkalk»	558	2	1	3	2	0	2
	8	«Felsenkalke»/ «Massenkalk»	577.7	2	1	2	1	0	2
	9	Wildegg Fm.	767.2	No	1	3	3	0	No
	10	Schwarzbach Fm.	666.4	No	1	0	2	1	2
4 (Run 4.4.2)	1	Klettgau Fm.	1'044.8	2	1	1	1	2	2
	2	Klettgau Fm.	1'051.52	2	0	0	0 (no rebound)	0	No
5 (Run 5.1.8)	1-1b	Weitenau Fm.	1'331.6	2	1	4	2	0	2
	1-2	Weitenau Fm.	1'329.6	2	1	2	0	1	2
	1-3	Weitenau Fm.	1'361.1	No	0	0	0	0	No
	2-1	Kaiseraugst Fm.	1'277.25	No	1	0	3 (+1 with breakdown)	1	2
	3-1	Zeglingen Fm.	1'226.25	2	0	0	0	0	No
	3-2	Zeglingen Fm.	1'218.3	2	1	2	1	2	2
	3-3	Zeglingen Fm.	1'242.5	2	1	1	0	0	2
	1-3	Weitenau Fm.	1'361.1	No	0	0	0	0	No

5.4 MHF results

20 tests were attempted, with 13 of them being successful, from the «Felsenkalke» / «Massenkalk» unit (~ 550 m) down to the Permo-Carboniferous Basement (~ 1'350 m). The state of the borehole wall did not allow stress testing of the Opalinus Clay. Tests without the ability to breakdown the formation or with an inability to maintain a high-pressure seal were deemed unsuccessful. Any other test where a closure stress could be estimated was deemed successful.

Tab. 5-2 presents a quicklook interpretation of the MHF results, which includes the “breakdown pressure”, the closure stress range and associated comments. The 'breakdown pressure' is taken as the maximum pressure reached during the first hydraulic fracturing cycle. A classical breakdown pressure interpretation should not be applied to these pressure values because sleeve fracturing was performed prior to hydraulic fracturing. Recorded 'breakdown pressures' are therefore technically reopening pressures. The closure stress acts normal to the fracture surface. Its range was determined from the pressure records and expressed with a lower and an upper bound.

Fig. 5-3 plots the closure stress ranges from the quicklook analysis as a function of depth together with the overburden vertical stress (Sv), estimated from integration of the density logs over depth, and the maximum pressures measured during the formation integrity tests (FIT).

Quicklook analysis of the post-MHF borehole imagery showed that new or enhanced features (longitudinal) could be observed at successful station locations. Conversely, in unsuccessful tests, no new feature could be observed. Fig. 5-4 presents the pre- and post-MHF images for Station 10 (Run 2.6.2). New fracture traces induced by the MHF test are shown with blue arrows on the rightmost track. The trace of the new fracture traces is reported in red on the first FMI track to show that, even with the incomplete borehole coverage of the pre-MHF image, the pre-MHF image shows that the formation was not fractured prior to MHF. A comparison of all the pre- and post-MHF borehole images is included in Appendix D.

Interpretation of sleeve fracturing/sleeve reopening tests was not performed as part of the acquisition program and is not included in this report.

Tab. 5-2: Quicklook interpretation of MHF results for the BUL1-1B borehole

Section Run Diameter	**Station**	**Formation**	**Depth** (m MD)	**Breakdown pressure** (MPa)	**Closure stress range** (MPa)	**Comments**
2 Run 2.6.2 6 3/8" bit size	7	«Felsenkalke» / «Massenkalk»	558	20.75	11.4 – 14.0	Possibly Shmin
	8	«Felsenkalke» / «Massenkalk»	577.7	24.8	12.4 – 14.3	Possibly Shmin
	10	Schwarzbach Fm.	666.4	16.1	11.5 – 14.5	Stress assignment unclear
	6	Schwarzbach Fm.	668.4	35.45	16.3 – 19.35	Shmin likely
	1	Wildegg Fm.	765.25	> 41*	N/A	No breakdown achieved
	9	Wildegg Fm.	767.2	18.15 (max. pressure)	13.2 – 15.8	HTPF, but a new longitudinal feature may also have been created
	2	Wildegg Fm.	772.4	> 41*	N/A	No breakdown achieved
	5	«Herrenwis Unit»	814.4	22.75	14.3 – 16.6	Shmin likely
	3	«Herrenwis Unit»	847.1	17.8	12.7 – 14.8	Shmin likely
	4	Wedelsandstein Fm.	871.2	> 41*	N/A*	No breakdown achieved
4 Run 4.4.2 6 3/8 bit size	1	Klettgau Fm.	1'044.8	24.2	15.8 – 17.5	Shmin likely
	2	Klettgau Fm.	1'051.52	27.6*	N/A	High pressure leaks only
5 Run 5.1.8 6 3/8 bit size	3-2	Zeglingen Fm.	1'218.3	37.3	24.5 – 25.5	Shmin likely
	3-1	Zeglingen Fm.	1'226.25	> 41*	N/A	No breakdown achieved
	3-3	Zeglingen Fm.	1'242.5	43.9	33.75 – 34.5	Shmin likely
	2-1	Kaiseraugst Fm.	1'277.25	26.9	23.4 – 26.9	Shmin likely
	1-2	Weitenau Fm.	1'329.6	42.9	30.0 – 32.0	Possibly Shmin (Sv?)?
	1-1b	Weitenau Fm.	1'331.6	39.22	26.0 – 28.0	Shmin likely
	1-3	Weitenau Fm.	1'361.1	37.23*	N/A	No breakdown achieved High pressure leaks
Total number of tests						20
Total number of successful tests						13
Success rate						65%

* If no hydraulic fracture could be created, the maximum pressure applied to the interval was provided.

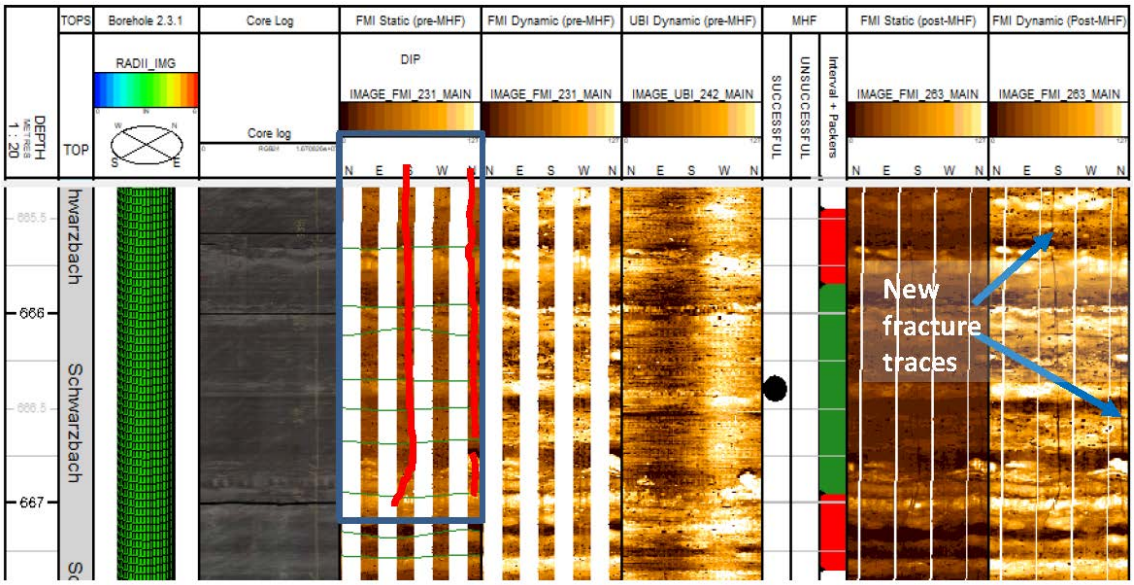

Fig. 5-3: Example of pre- vs post-MHF images (pre-MHF images are presented on the left of the MHF columns

Post-MHF images are presented on the right.

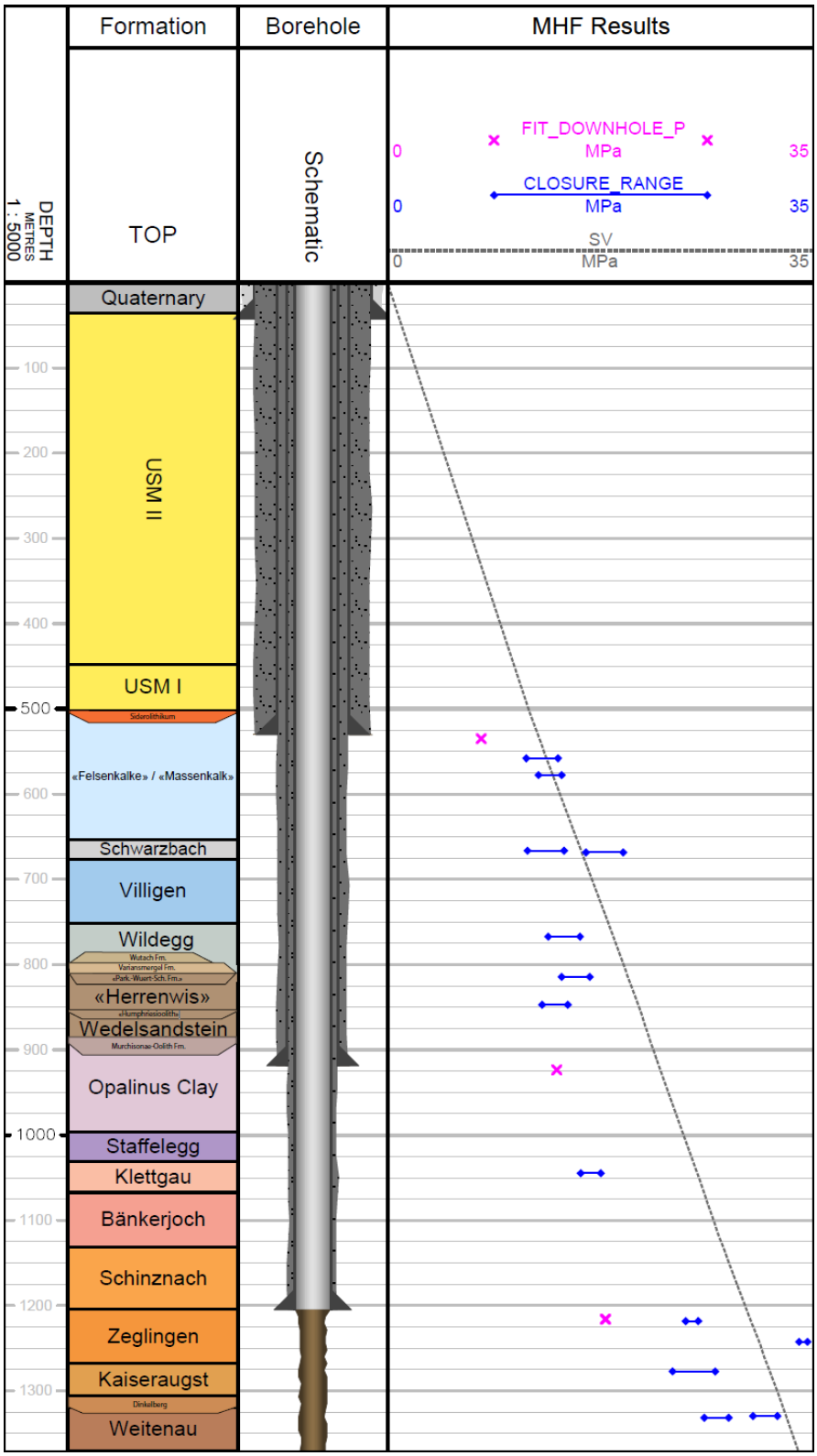

Fig. 5-4: Comparison of the quicklook closure stress range obtained from the MHF tests with the overburden vertical stress (Sv) from the integration of density over depth and the maximum pressures attained during the formation integrity tests (FIT)

6 References

Bérard, T. & Prioul, R. (2016): Mechanical Earth Model. Oilfield Review: The Defining Series , https://www.slb.com/resource-library/oilfield-review/defining-series/defining-mem.

Desroches, J. & Kurkjian, A.L. (1999): Applications of Wireline Stress Measurements. Paper SPE-58086, SPE Reservoir Evaluation & Engineering, 2(5), 451-461. DOI:10.2118/ 58086-PA.

Haimson, B.C. (1993): The Hydraulic Fracturing Method of Stress Measurement: Theory and Practice, Chapter 14, in Hudson, J., Editor, Comprehensive Rock Engineering, 3, 395-412, Pergamon Press. DOI: 10.1016/B978-0-08-042066-0.500215.

Haimson, B.C. & Cornet, F.H. (2003): ISRM Suggested Methods for Rock Stress Estimation – Part 3: Hydraulic Fracturing (HF) and/or Hydraulic Testing of Pre-Existing Fractures (HTPF), International Journal Rock Mechanics and Mining Sciences, 40(7-8), 1011-1020. DOI: 10.1016/j.ijrmms.2003.08.002.

Isler, A., Pasquier, F. & Huber, M. (1984): Geologische Karte der zentralen Nordschweiz 1:100'000. Herausgegeben von der Nagra und der Schweiz. Geol. Komm.

Nagra (2014): SGT Etappe 2: Vorschlag weiter zu untersuchender geologischer Standortgebiete mit zugehörigen Standortarealen für die Oberflächenanlage. Geologische Grundlagen. Dossier II: Sedimentologische und tektonische Verhältnisse. Nagra Technischer Bericht NTB 14-02.

Pietsch, J. & Jordan, P. (2014): Digitales Höhenmodell Basis Quartär der Nordschweiz – Version 2013 (SGT E2) und ausgewählte Auswertungen. Nagra Arbeitsbericht NAB 14-02.

Plumb, R., Edwards, S., Pidcock, G., Lee, D. & Stacey, B. (2000): The Mechanical Earth Model Concept and Its Application to High-Risk Well Construction Projects. SPE Paper #59128 presented at the IADC/SPE Drilling Conference, New Orleans, Louisiana, February 2000. doi: https://doi.org/10.2118/59128-MS.

Schlumberger (2013): Log Interpretation Charts, https://www.slb.com/resource-library/book/log-interpretation-charts.

Serra, O. E. (1983): Fundamentals of well-log interpretation.

Wileveau, Y., Cornet, F.H., Desroches, J. & Blumling, P. (2007): Compelte in sit stress determination in an argillite sedimentary formation, Physics and chemistry of the Earth Parts A/B/C 32(8-14):866-878. DOI: 10.1016/j.pce.2006.03.018.